

Copy No. 107

RM No. L8D06

NACA RM No. L8D06

C/

@ /



RESEARCH MEMORANDUM

EFFECT OF HIGH-LIFT DEVICES ON THE LONGITUDINAL AND LATERAL
CHARACTERISTICS OF A 45° SWEPTBACK WING WITH
SYMMETRICAL CIRCULAR-ARC SECTIONS

By

Eugene R. Guryansky and Stanley Lipson

Langley Aeronautical Laboratory
Langley Field, Va.

CLASSIFIED DOCUMENT

This document contains classified information affecting the National Defense of the United States within the meaning of the Espionage Act, USC 50:31 and 32. Its transmission or the revelation of its contents in any manner to an unauthorized person is prohibited by law. Information so classified may be imparted only to persons in the military and naval services of the United States, appropriate civilian officers and employees of the Federal Government who have a legitimate interest therein, and to United States citizens of known loyalty and discretion who of necessity must be informed thereof.

ENGINEERING DEPT. LIBRARY
CHANCE VUGHT AIRCRAFT
STRATFORD, CONN.

NATIONAL ADVISORY COMMITTEE
FOR AERONAUTICS

WASHINGTON
October 1, 1948

RM L8D06

10/6/48

NATIONAL ADVISORY COMMITTEE FOR AERONAUTICS

RESEARCH MEMORANDUM

EFFECT OF HIGH-LIFT DEVICES ON THE LONGITUDINAL AND LATERAL
CHARACTERISTICS OF A 45° SWEEPBACK WING WITH
SYMMETRICAL CIRCULAR-ARC SECTIONS

By Eugene R. Guryansky and Stanley Lipson

SUMMARY

An investigation has been conducted in the Langley full-scale tunnel to determine the longitudinal characteristics of several leading-edge and trailing-edge flap configurations and the lateral characteristics of one flapped configuration of a 45° sweptback wing having circular-arc sections, an aspect ratio of 3.5, and a taper ratio of 0.5. Tests were also made of chordwise fences with and without a rounded leading-edge modification installed on the outer semispan of the wing in an attempt to alleviate the early tip stall. All the test results are presented for a Reynolds number of 4.5×10^6 .

The maximum lift coefficient is 0.87 for the wing with flaps neutral, 1.07 with the full-span leading-edge flap deflected 40° (not completely stalled), 1.05 with the full-span trailing-edge flap deflected 40° , and 1.26 with the combination of the two flap configurations. None of the configurations investigated provided completely satisfactory longitudinal stability characteristics throughout the entire lift-coefficient range. Some improvement in the longitudinal characteristics of the wing in the moderate to high lift-coefficient range is provided by the leading-edge flaps.

No appreciable improvement in the stability of the wing at stall is realized as a result of the installation of either the outer semispan rounded leading edge or of the chordwise fences or of a combination of these two configurations. With the full-span leading-edge flap deflected 40° and with the semispan trailing-edge flap deflected 60° the wing has positive effective dihedral throughout the angle-of-attack range of the tests and attains a maximum C_{l_ψ} value of 0.0036 per degree at a lift coefficient of 0.96. The wing is directionally stable for this flap configuration and reaches a maximum C_{n_ψ} value of about -0.001 at a lift coefficient of 0.97.

For a representative wing loading, 40 pounds per square foot at sea level, high gliding and sinking speeds are characteristic of this wing for all the flap configurations tested.

ENGINEERING DEPT. LIBRARY
CHANCE VUGHT AIRCRAFT
STRATFORD, CONN.

INTRODUCTION

As a part of the general investigation of the landing characteristics of wings for transonic and supersonic airplanes, tests have been made in the Langley full-scale tunnel to determine the aerodynamic characteristics of wings with several different plan forms having circular-arc sections. A previous paper (reference 1) presents the aerodynamic characteristics of a 45° sweptback wing having a taper ratio of 0.5 and an aspect ratio of 3.5. This paper contains the longitudinal characteristics for a number of 0.20c plain leading-edge and trailing-edge flap configurations and the lateral characteristics for one flapped arrangement of the aforementioned wing. Also determined was the effectiveness of several combinations of chordwise fences and of a rounded leading edge installed on the outer semispan in alleviating the inherently poor stalling characteristics of this type of wing (references 1 and 2). All the tests were made at a Reynolds number approaching the full-scale value for a small fighter-type airplane and at a Mach number low enough so that compressibility effects were negligible.

COEFFICIENTS AND SYMBOLS

The data are referred to the stability axes, which are a system of axes in which the Z-axis is in the plane of symmetry and perpendicular to the relative wind, the X-axis is in the plane of symmetry and perpendicular to the Z-axis, and the Y-axis is perpendicular to the plane of symmetry. The origin was located at the quarter-chord point of the mean aerodynamic chord. The positive directions of forces, of moments, and of angular displacements of the model are given in figure 1.

C_L	lift coefficient	$\left(\frac{\text{Lift}}{qS}\right)$
C_D	drag coefficient	$\left(\frac{D}{qS}\right)$
C_Y	lateral-force coefficient	$\left(\frac{Y}{qS}\right)$
C_m	pitching-moment coefficient	$\left(\frac{M}{qSc}\right)$
C_n	yawing-moment coefficient	$\left(\frac{N}{qSb}\right)$
C_l	rolling-moment coefficient	$\left(\frac{L}{qSb}\right)$
D	drag, pounds	

Y	lateral force, pounds
M	pitching moment about Y-axis, positive when moment tends to increase angle of attack, foot-pounds
N	yawing moment about X-axis, positive when moment tends to retard right wing panel, foot-pounds
L	rolling moment about X-axis, positive when moment tends to raise left wing panel, foot-pounds
C_{l_ψ}	rate of change of rolling-moment coefficient with angle of yaw, per degree $\left(\frac{\partial C_l}{\partial \psi}\right)$
C_{n_ψ}	rate of change of yawing-moment coefficient with angle of yaw, per degree $\left(\frac{\partial C_n}{\partial \psi}\right)$
C_{Y_ψ}	rate of change of lateral-force coefficient with angle of yaw, per degree $\left(\frac{\partial C_Y}{\partial \psi}\right)$
q	free-stream dynamic pressure, pounds per square foot $\left(\frac{1}{2}\rho V^2\right)$
V	free-stream velocity, feet per second
S	wing area, 231 square feet
b	wing span, 28.5 feet
\bar{c}	mean aerodynamic chord measured parallel to plane of symmetry, 8.37 feet $\left(\frac{2}{S} \int_0^{b/2} c^2 dy\right)$
\bar{x}	distance from leading edge of root chord to quarter chord of the mean aerodynamic chord, 9.03 feet $\left(\frac{2}{S} \int_0^{b/2} cx dy\right)$
R	Reynolds number $\left(\frac{V\bar{c}}{\gamma}\right)$
α	angle of attack measured in plane of symmetry, degrees
ψ	angle of yaw, positive when right wing panel is retarded, degrees
δ	angle of flap deflection, degrees
γ	kinematic viscosity, square feet per second

- c chord, parallel to plane of symmetry, feet
- x longitudinal distance, parallel to plane of symmetry, from leading edge of root chord to quarter-chord point of each section, feet
- λ taper ratio, 0.5, $\left(\frac{\text{tip chord}}{\text{root chord}} \right)$
- A aspect ratio, 3.5, $\left(\frac{b^2}{s} \right)$
- c' chord, perpendicular to line of maximum thickness, feet

DESCRIPTION OF WING

The plan form of the wing showing some of the more significant details and dimensions is presented in figure 2. The wing has an angle of sweepback of 45° at the quarter-chord line, an aspect ratio of 3.5, a taper ratio of 0.5, and has no geometric dihedral or twist. The airfoil sections perpendicular to the line of maximum thickness are biconvex sections (NACA 2S-50(05)-50(05)) with the maximum thickness of 10-percent chord at the 50-percent chord line. A detailed description of the wing construction is contained in reference 1.

The wing is equipped with both leading-edge and trailing-edge full-span 20-percent-chord plain flaps. These leading-edge and trailing-edge flaps were made in four and two equal spanwise sections, respectively, as shown in figure 2, and could be deflected individually or in any desired combination. The flaps were hinged on the lower surface and, when deflected, produced a gap on the upper surface which was covered and faired by sheet-metal seals and modeling clay.

As part of the investigation, tests were made of boundary-layer-control fences and of a wooden glove which refaired the forward 50 percent of the wing chord from the circular-arc section to the elliptical contour shown in figure 3. The latter configuration will be referred to in the text as the rounded leading edge. The glove was installed on the outer semispan of the wing panels and the finish was aerodynamically smooth. The rear part of the glove faired smoothly into the basic contour of the wing at the line of maximum thickness. The inboard end of the glove, however, was not faired into the wing and a discontinuity in the wing surface resulted as shown in figure 3. The shape and dimensions of the fences tested are shown in figure 4. The fences were aligned with the air stream and installed at both the 50-percent and the outboard 75-percent semispan stations.

TESTS

The wing was supported on the six-component tunnel balance as shown in figure 5. Forces and moments in pitch were measured for various

deflections of the leading-edge and trailing-edge flaps through an angle-of-attack range between -0.1° and 26° . For the configuration with the full-span leading-edge flap at 40° and the semispan trailing-edge flap at 60° , tests were also conducted through a yaw range from -2.5° to 6° .

Stall studies were made both visually and from photographic records of the behavior of wool tufts attached to the upper surface of the wing at suitable stations so as to indicate the entire flow pattern.

A few tests were made through a range of Reynolds number from 2.2×10^6 to 6.5×10^6 to determine the scale effect on the aerodynamic characteristics of the unyawed wing with flaps deflected. The majority of the tests, however, were run at a Reynolds number of 4.5×10^6 .

RESULTS AND DISCUSSION

The data presented herein, except for the rolling-moment and yawing-moment coefficients, have been corrected for wing-support tares, interference effects, and air-stream misalignment with the jet-boundary corrections being calculated on the basis of an unswept wing. All these corrections have been determined for the zero yaw condition.

Since the results of the tests to determine scale effect with flaps deflected showed that there was practically no Reynolds number effect, all test results reported herein are given for a Reynolds number of 4.5×10^6 .

The discussion is divided into seven sections under the following headings: Stall Studies, Leading-Edge Flaps, Trailing-Edge Flaps, Flap Combinations, Rounded Leading-Edge Modification and Fences, Landing-Performance Characteristics, and Aerodynamic Characteristics in Yaw.

Stall Studies

The tuft studies showing the stall progression for the basic wing with flaps neutral (fig. 6) reveal that even at low lift coefficients the flow at the wing tips is very rough and that the boundary layer at the leading edge flows strongly outward toward the tips. Stall at the wing tips is well developed at a lift coefficient of 0.4, and as the angle of attack is increased the stall progresses inboard.

An improvement in the wing-tip-flow conditions at low lift coefficients was obtained by deflecting the outboard $0.25\frac{b}{2}$ section of the leading-edge flap 30° (fig. 7). This effect is reduced as the lift coefficient is increased, however, so that at a lift coefficient of about 0.8 the flow characteristics resemble those for the basic wing.

The effect of deflecting the inboard semispan trailing-edge flap 60° in combination with the outboard $0.25\frac{b}{2}$ leading-edge flap deflected 30° is shown in figure 8. As compared with the plain wing, the onset of tip stall is delayed, in general, to a higher lift coefficient ($C_L \approx 0.7$). At maximum lift, except for a slight decrease in the steadiness of the flow at the center part of the wing, the flow pattern is not essentially altered by this combination of flap deflections.

The stall patterns obtained with additional sections of the leading-edge flap deflected are shown in figures 9 and 10. With the outboard 50 percent of the leading-edge flap deflected 30° and with the inboard semispan trailing-edge flap deflected 60° the tip sections are essentially unstalled up to about $C_{L_{max}}$. The stall originates at the inboard end of the deflected leading-edge flap at a C_L of about 0.9 and progresses inboard and outboard at approximately the same rate until the wing is stalled. When the outboard 75 percent of the leading-edge flap was deflected 30° in conjunction with the inboard semispan trailing-edge flap deflected 60° (fig. 10), the initial wing stall was delayed to very high angles of attack ($C_L \approx 1.0$). The smooth flow over the outer part of the wing, however, was attained at the expense of having the initial stall appear once again at the tips.

Leading-Edge Flaps

The aerodynamic characteristics of the wing tested with various leading-edge flap configurations and with the trailing-edge flaps retracted are given in figure 11. The results presented in figure 11(a) are for the conditions with the full-span leading-edge flaps deflected through a range of angle from 0° to 40° in 10° increments. A 23-percent increase in lift coefficient above the maximum lift coefficient for the plain wing (0.87) is realized with the full-span leading-edge flap deflected 40° . The results for the 40° flap configuration showed an increase in lift coefficient at the highest angle of attack only 2 percent greater than that for the 30° deflection; therefore, full-span leading-edge flap deflections greater than 40° were not tested. It is probable that the increased bend at the 0.20c' station associated with the large flap deflections produces a comparatively large pressure peak which induces flow separation over the forward part of the airfoil. It should be mentioned that in several instances maximum lift was not actually attained due to limitations of the apparatus which prevented increasing the angle of attack above 26° . Results of tests with different sections of the leading-edge flap deflected 20° and 30° are presented in figures 11(b) and 11(c). The deflection of the outboard 25 percent of the flap makes no appreciable change in the maximum lift coefficient of the plain wing for either of these two deflections. With the outboard 50 percent of the flap deflected 20° and 30° , however, the lift coefficient at the highest angle of attack attained is increased 6 percent and 17 percent, respectively. Further increases are obtained when the outboard

75 percent of the flap is deflected, but for a spanwise length greater than 75 percent, very little gain in lift coefficient is realized.

The deflection of the full-span leading-edge flap increases the drag coefficient slightly up to a lift coefficient of about 0.3 but decreases it at all greater lift coefficients. With the full-span leading-edge flap deflected 40° , the decrease in drag coefficient at a lift coefficient of 0.85 is 67 percent of the drag coefficient for the base condition. A similar effect is obtained when sections of the leading-edge flap are deflected and the magnitude of the drag decreases with increases in the span of the deflected flap.

The variations of pitching-moment coefficient with lift coefficient and with angle of attack are also shown in figure 11. With flaps retracted, the wing is neutrally stable to a lift coefficient of 0.3, then slightly stable to 0.55, and finally unstable to the maximum lift coefficient with a stable break occurring at the stall. The shapes of the pitching-moment curves for the wing with the full-span flap deflected are similar to those for the plain wing up to a lift coefficient of about 0.5. The effect of deflecting the leading-edge flap is to delay the onset of the instability of the wing to higher lift coefficients; the lift coefficients at which this instability occurred increased with an increase in the angle of flap deflection. Deflecting the outboard $0.25\frac{b}{2}$ of the leading-edge flap increased the stability of the wing in the higher lift-coefficient range and provided a stable break past the stall similar to that obtained with the basic wing. Increasing the deflected leading-edge flap span to $0.50\frac{b}{2}$ and $0.75\frac{b}{2}$ produced still greater increases in stability in the higher lift-coefficient range but gave an unstable break past the stall.

Trailing-Edge Flaps

The effects of semispan and full-span trailing-edge flap deflection on the characteristics of the wing are shown in figures 12(a), 12(b), and 12(c).

The inboard semispan flap contributes approximately one-half the increment in $C_{L_{max}}$ obtained with the full-span trailing-edge flap deflected 20° , as shown in figure 12(a), but produces a much greater percentage of the total increment at angles of attack below that for $C_{L_{max}}$. Figure 12 shows that the $C_{L_{max}}$ obtained with the inboard semispan flap deflected is the same value ($C_{L_{max}} \approx 0.93$) for the test range of flap deflection. The effectiveness of the full-span flap is slightly increased from 20° to 40° ($C_{L_{max}}$ of 1.01 as compared with 1.05), but a further increase in the full-span flap deflection fails to produce any further increase in $C_{L_{max}}$. At low angles of attack, deflecting the trailing-edge flap produces large increments of lift but the effectiveness decreases rapidly as maximum lift is approached.

Deflection of the trailing-edge flap results in significant drag reductions above lift coefficients of 0.60 as compared with that for the basic wing. The effect of this drag reduction produced by the trailing-edge flaps on the landing-performance characteristics of the wing will be discussed later in the report.

The shape of the $C_m - C_L$ curve for the plain wing is not greatly altered by deflection of either the semispan or full-span trailing-edge flaps. The neutrally stable portion of the curve is extended to higher lift coefficients and is then followed by a severe decrease in longitudinal stability up to maximum lift. At the stall, a stable break in the pitching-moment curve occurs for all of the trailing-edge flap configurations tested.

Flap Combinations

The results for the combinations of leading-edge and trailing-edge flap deflections are shown in figure 13. Figures 13(a) to 13(d) present the results of various full-span trailing-edge flap deflections for a range of full-span leading-edge flap deflections from 10° through 40° . Figures 13(e) and 13(f) show the results obtained with the inboard semispan flaps deflected 60° in combination with a number of leading-edge flap configurations.

As shown in figures 13(a) to 13(d), the effectiveness of either the full-span leading-edge or trailing-edge flap is unaffected by the presence of the other flap when tested in combination. The increment in maximum lift coefficient produced by the various flap combinations, therefore, is approximately equal to the sum of the lift-coefficient increments contributed by the individual flaps. As previously discussed, at a given lift coefficient (above $C_L = 0.60$) and with the trailing-edge flaps neutral, increasingly large drag reductions were obtained by deflecting the full-span leading-edge flap. When the leading-edge flap is operated in combination with the trailing-edge flap, however, this effect is materially reduced with the magnitude of the drag reductions becoming less with increasing trailing-edge-flap angle. The configuration with both the full-span leading-edge and trailing-edge flaps at high deflections produced increases in the longitudinal stability in the lower lift-coefficient range. For all the flap combinations tested, the pitching-moment breaks at the stall are unstable.

The effects of deflecting sections of the leading-edge flap 30° with the inboard 50 percent of the trailing-edge flap deflected 60° are shown in figure 13(e). Deflection of the outboard 25 percent of the leading-edge flap produces no effect on the maximum lift coefficient, but deflection of the outboard 50 percent, outboard 75 percent, and full span of the leading-edge flap increases the $C_{L_{max}}$ of the wing by increments of 0.13, 0.23, and 0.18, respectively.

With the inboard semispan trailing-edge flap deflected 60° , as the span of the leading-edge flap was increased from $0.25\frac{b}{2}$ to full span, the drag of the wing at the higher lift coefficients was proportionally decreased. The effect of deflecting the outboard quarter and the outboard half of the leading-edge flap with the inboard semispan flap deflected 60° is to increase the longitudinal stability of the wing at the higher angles of attack. As indicated by the stall studies (fig. 10), deflection of the outboard 75 percent of the leading-edge flap changes the flow characteristics of the wing. With this configuration tip stalling appears before any central portion of the wing is completely stalled, thereby making the wing highly unstable at angles of attack from 20° through 26° . Deflection of the full-span leading-edge flap results in neutral longitudinal stability of the wing up to the stall and an unstable break beyond this point.

The effect of deflecting the full-span leading-edge flap in combination with the semispan trailing-edge flap deflected 60° is presented in figure 13(f). Practically the full effectiveness of the leading-edge flap was realized at a flap deflection of 30° .

A comparison of figure 13(f) with figures 13(c) and 13(d) indicates that the effectiveness of the semispan trailing-edge flap as compared with the full-span flap remains the same for the leading-edge flap neutral or deflected. (See fig. 12(c).) The combination of the semispan trailing-edge flap deflected 60° and the full-span leading-edge flap deflected 30° or 40° does not produce the increases in stability in the low lift-coefficient range as is obtained when the entire span of the trailing-edge flap is deflected 60° .

Rounded Leading-Edge Modification and Fences

The results for the basic wing show that a strong spanwise flow toward the tips results in early tip stall at an angle of attack of about 7.5° . The results of tests made in an attempt to alleviate this condition by the use of a rounded leading-edge modification with and without full-chord fences are given in figures 14 to 16 and by the use of fences alone, in figures 17 and 18.

A considerable reduction in the spanwise flow over the rounded leading edge and an improvement in the flow at the wing tip results from the installation of the leading-edge modification (fig. 14). As discussed in the section entitled "Description of Wing," there was a jog in the spanwise contour of the wing with the rounded leading edge installed. This discontinuity may have acted as a very small boundary-layer-control fence. Unpublished data, however, indicate that a fence of this maximum height (0.0122c') has a negligible effect on the spanwise flow. This leading-edge modification delays the appearance of intermittent stall at the tip to an angle of attack of about 14.5° , or 7° beyond that for

the basic wing. However, the progression of the stall was rapidly inboard from the tips with further increases in angle of attack so that at the angle for maximum lift a large portion of the outer semispan of the wing was stalled in a manner similar to the basic wing.

The aerodynamic characteristics for the basic wing and for the wing modified with the rounded leading edge are presented in figure 15. The data show that (a) the maximum lift coefficients for these two configurations are approximately equal, (b) the lift curve is more linear for the rounded leading-edge configuration, and (c) only small differences exist in the drag and the pitching characteristics.

The stalling characteristics resulting from the addition of full-chord fences, located at the $0.50\frac{b}{2}$ stations, to the wing with the rounded leading edge are presented in figure 16. The fences effectively eliminate the spanwise boundary-layer flow to such an extent that the stall is delayed to nearly the angle of maximum lift. However, the wing section adjacent to the inboard side of the fences stalls intermittently at lower angles of attack and this stall slowly progresses inboard with further increases in angle of attack.

The aerodynamic characteristics of the wing obtained with the rounded leading-edge configuration with the $0.50\frac{b}{2}$ station fences is presented in figure 17. These fences increase the static longitudinal stability of the wing with the rounded leading edge up to a C_L of 0.8 (see figs. 15 and 17) by eliminating the tip stall and by inducing stall inboard of the fence location. However, with further increases in angle of attack, the outboard section of the wing stalls rapidly and produces a sharp unstable break in the pitching-moment curve at the angle for maximum lift. There is essentially no effect of the fences on the lift characteristics of the wing with the rounded leading edge except for a slight $C_{L_{max}}$ reduction from 0.88 to 0.86. (See figs. 15 and 17.) The fences cause a small reduction in drag at the higher angles of attack.

The installation of the full-chord fences at the $0.50\frac{b}{2}$ stations on the basic wing produced results that were quite similar to those obtained for the configuration with the fences and the rounded leading edge (fig. 17). The maximum lift of the two configurations is about the same, but the drag was higher for the basic wing at the lower lift coefficients (below $C_L = 0.8$). The basic wing with fences is somewhat more stable in the lower range of lift coefficient, but both test arrangements have unstable pitching-moment breaks at the stall.

The effect of an additional set of full-chord fences located at the outboard $0.75\frac{b}{2}$ stations on the aerodynamic characteristics of the wing with fences at the $0.50\frac{b}{2}$ stations is shown in figure 18. The maximum lift coefficient and drag of the basic wing are slightly reduced by the

addition of either fence arrangement. The wing with any of the fence arrangements installed has a stable pitching-moment slope from $C_L = 0.4$ to $C_L = 0.7$ which is quite similar to that obtained for the rounded leading-edge installation. A sharp unstable break in the pitching-moment curve occurs, however, at angles of attack just below maximum lift with the fences installed.

Landing-Performance Characteristics

In order to evaluate the effect of various flap arrangements on the landing performance of this wing, a comparison of the sinking-speed - gliding-speed variations is presented for a few of the configurations. The results (fig. 19) are plotted as lift-drag polars upon which are superimposed lines of constant sinking and gliding speeds computed for a wing loading of 40 pounds per square foot at sea level. In order to compare more readily the landing characteristics of the five configurations, the results are presented in figure 20 as a plot of sinking speed against gliding speed.

It is apparent from these results (see fig. 20) that it is quite difficult to obtain a reasonable value of sinking speed in conjunction with a low landing speed. The only configuration that meets the recommended sinking-speed criterion of 25 feet per second (reference 3) is the one with the leading-edge flap deflected 40° , but this figure is attained at a relatively high gliding speed of 134 miles per hour. For gliding speeds less than 127 miles per hour the combination of the leading-edge flap at 40° and the semispan trailing-edge flap at 60° gave the lowest total drag of the other flapped configurations so that at 120 miles per hour the sinking speed is about 31 feet per second. The attainment of greater maximum lift or lower glide speeds can be obtained by deflecting the full-span trailing-edge flap, but there is a simultaneous increase in drag resulting in very high sinking speeds.

Aerodynamic Characteristics in Yaw

The aerodynamic characteristics of the wing with the full-span leading-edge flap deflected 40° and the inboard semispan trailing-edge flap deflected 60° were determined for a limited range of yaw angle. This particular configuration was yawed because it produced a high value for $C_{L_{max}}$ and because it simulated a production configuration that could utilize conventional ailerons. The slopes of the C_l , C_n , and C_y against ψ curves were determined at 0° angle of yaw and are shown plotted against lift coefficient in figure 21. For comparative purposes, figure 21 also contains the lateral stability parameters obtained for the unflapped condition (reference 1).

The wing for this flapped configuration has a positive dihedral effect that increases from 0 at a lift coefficient of 0.23 to a maximum

value of C_{l_ψ} of 0.0036 per degree at a lift coefficient of 0.96 and then decreases to a value of 0.0025 at the highest lift coefficient tested ($C_L = 1.13$). The maximum value of C_{l_ψ} corresponds to an effective-dihedral angle of approximately 16° based on an unswept wing of aspect ratio 6, and of taper ratio 0.5 (reference 4). The reason for the large change in the lateral stability of the wing between the unflapped and flapped conditions is primarily concerned with the flow changes associated with the latter configuration. When the basic wing is yawed the forward panel tends to stall at a low lift coefficient and a strong destabilizing effect is produced. With the leading-edge flaps deflected, however, the tendency toward leading-edge stall at low lift coefficients is alleviated and the flow over the wing in yaw is then similar to the flow over wings with conventional sections.

The wing exhibits a decided increase of directional stability for this flap-deflected condition as compared with the undeflected condition of reference 1. The directional stability parameter C_{n_ψ} is negative throughout the test angle-of-attack range and decreases from 0 at a lift coefficient of 0.23 to about -0.001 per degree at a lift coefficient of 0.97 and then becomes less negative at higher lift coefficients.

SUMMARY OF RESULTS

The results of tests of a 45° sweptback wing with various high-lift and stall-control devices in the Langley full-scale tunnel are summarized as follows:

1. The maximum lift coefficients for the wing alone and for the most effective flap configurations are as follows:

(a) Wing alone	0.87
(b) Full-span leading-edge flap deflected 40° (not completely stalled).	1.07
(c) Full-span trailing-edge flap deflected 40°	1.05
(d) Combination of (b) and (c)	1.26

2. None of the configurations investigated provided completely satisfactory longitudinal stability characteristics throughout the entire lift-coefficient range. Some improvement in the longitudinal characteristics of the wing in the moderate to high lift-coefficient range is provided by the leading-edge flap.

3. The installation of a rounded leading edge on the outboard semispan section of the unflapped wing with or without boundary-layer-control fences improves the flow at the wing tips up to the stall but does not eliminate the unstable pitching tendency at the stall. The lift characteristics are not materially changed by these modifications.

4. For a representative wing loading, 40 pounds per square foot at sea level, high gliding and sinking speeds are a characteristic of this wing for all the test flap configurations.

5. With the full-span leading-edge flap deflected 40° and the semispan trailing-edge flap deflected 60° the wing has positive effective dihedral throughout the angle-of-attack range tested and attains a maximum value of C_{l_ψ} of 0.0036 per degree at a lift coefficient of 0.96.

6. The wing is directionally stable for this flap configuration and develops a maximum value of C_{n_ψ} of about -0.001 at a lift coefficient of 0.97.

Langley Aeronautical Laboratory
National Advisory Committee for Aeronautics
Langley Field, Va.

REFERENCES

1. Proterra, Anthony J.: Aerodynamic Characteristics of a 45° Swept-Back Wing with Aspect Ratio of 3.5 and NACA 2S-50(05)-50(05) Airfoil Sections. NACA RM No. L7C11, 1947.
2. Neely, Robert H., and Koven, William: Low-Speed Characteristics in Pitch of a 42° Sweptback Wing with Aspect Ratio 3.9 and Circular-Arc Airfoil Sections. NACA RM No. L7E23, 1947.
3. Gustafson, F. B., and O'Sullivan, William J., Jr.: The Effect of High Wing Loading on Landing Technique and Distance, with Experimental Data for the B-26 Airplane. NACA ARR No. L4KO7, 1945.
4. Pearson, Henry A., and Jones, Robert T.: Theoretical Stability and Control Characteristics of Wings with Various Amounts of Taper and Twist. NACA Rep. No. 635, 1938.

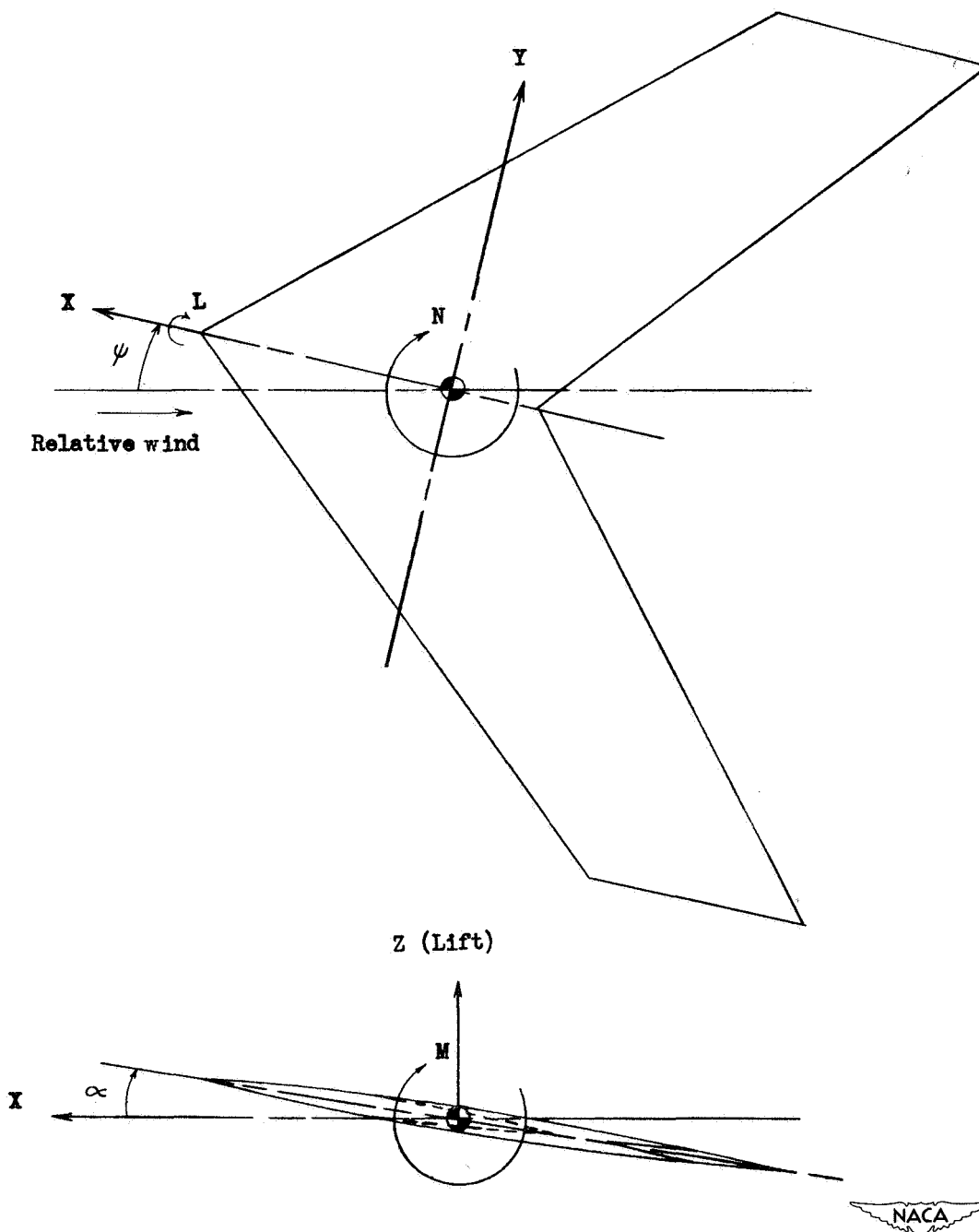


Figure 1. - System of axes. Positive values of forces, moments, and angles are indicated by arrows.

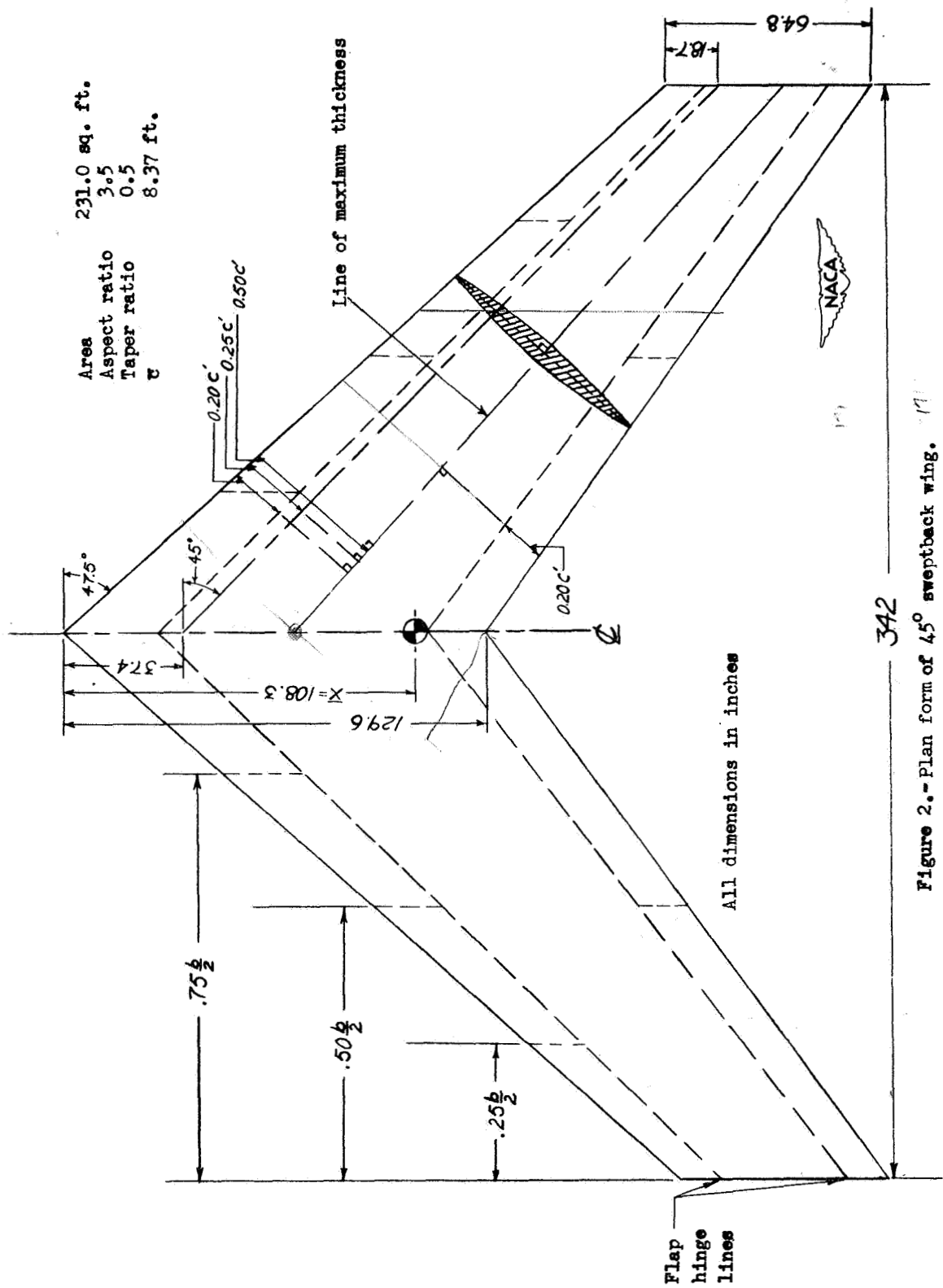


Figure 2.-Plan form of 45° sweptback wing.

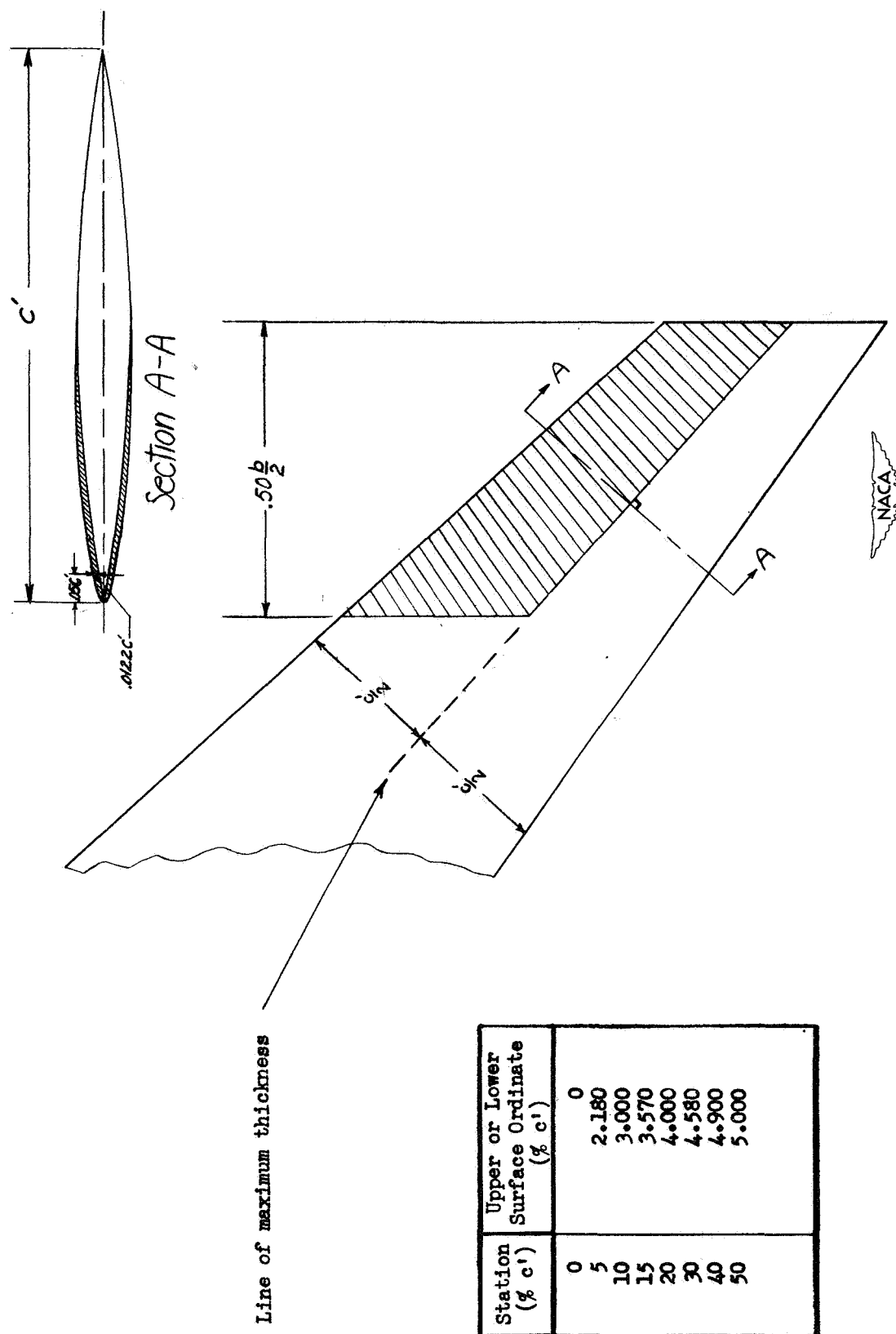
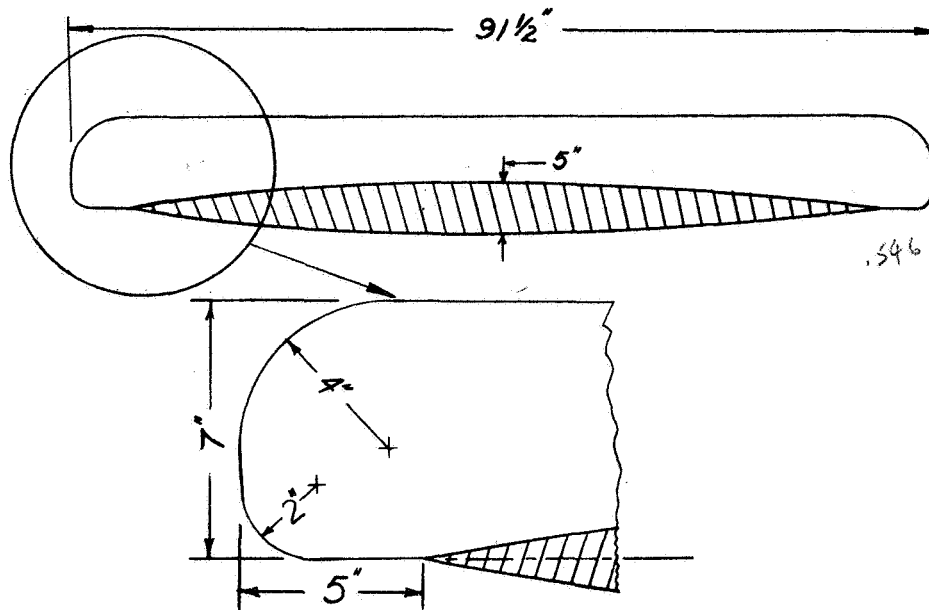
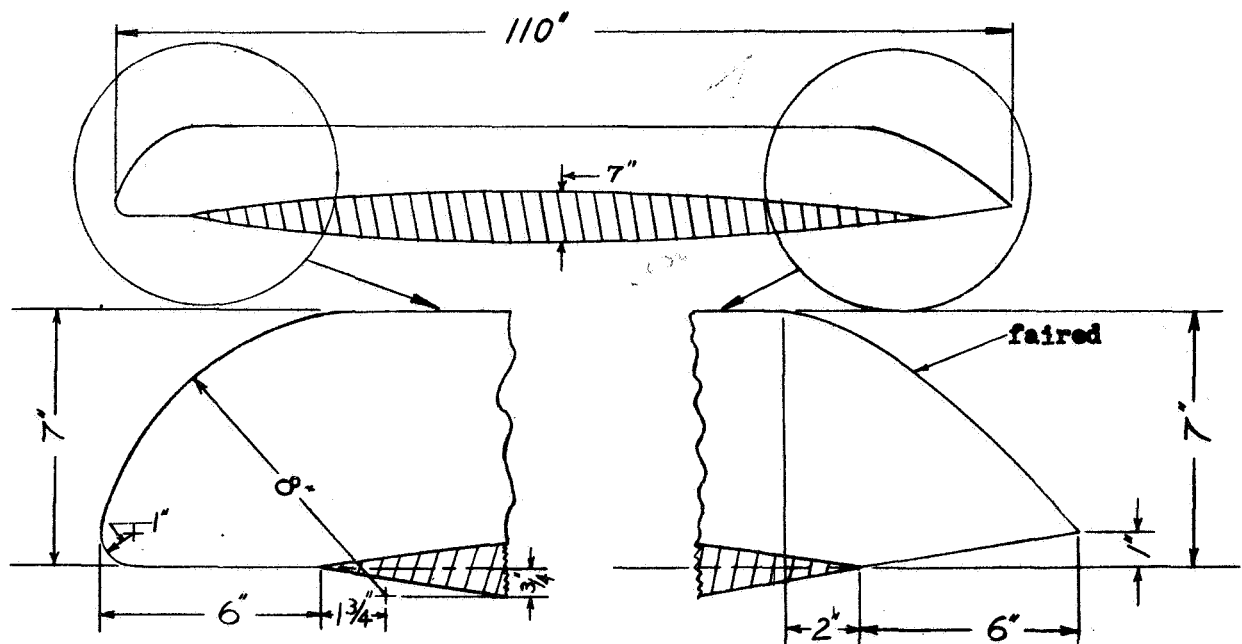


Figure 3. - Ordinates and location of the rounded leading edge as installed for the tests.



(a) Fence at the $.75b/2$ station
(not to scale).



(b) Fence at the $.50b/2$ station
(not to scale).



Figure 4.- Dimensions of the full chord fences. The stations refer to their spanwise location.

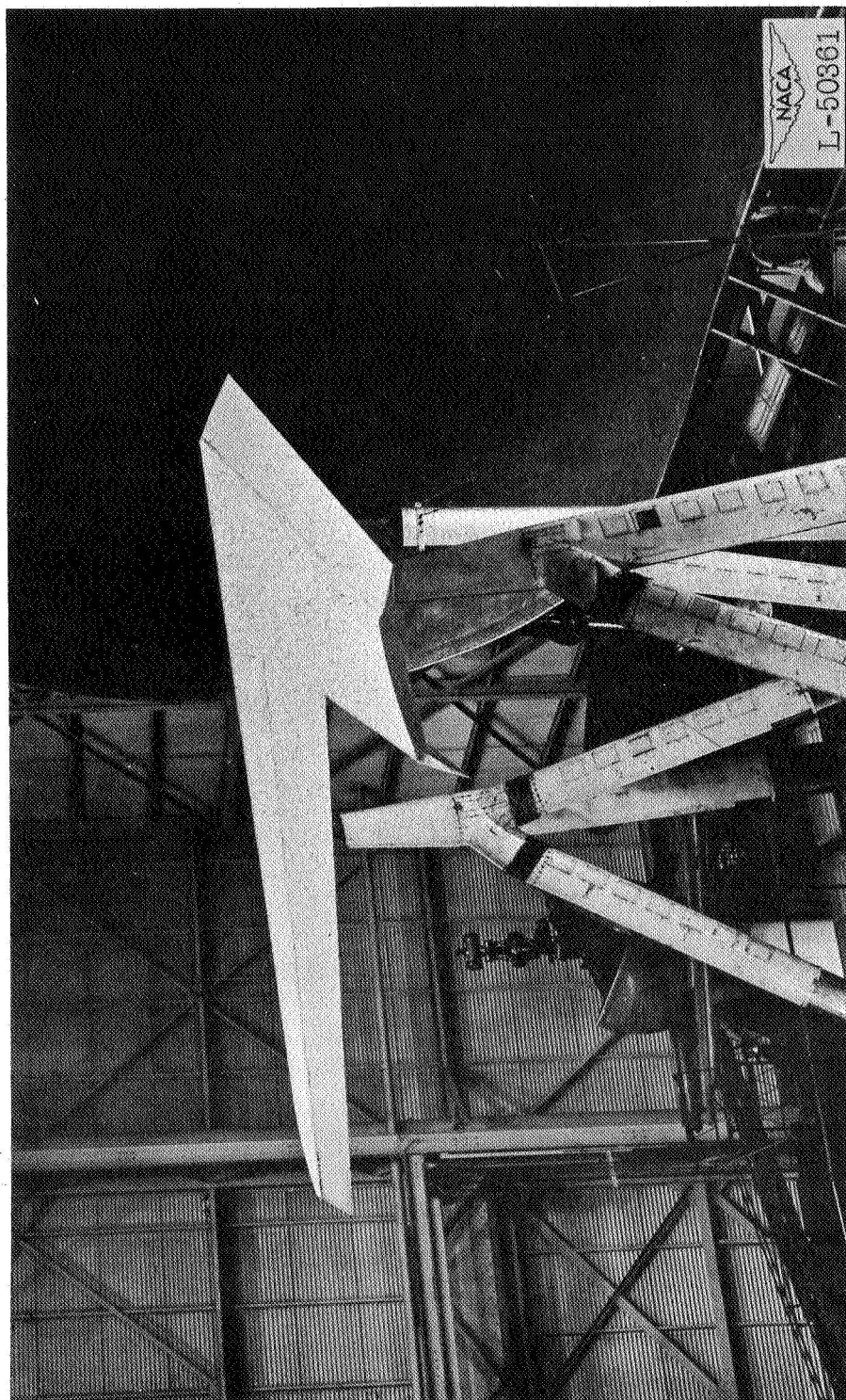


Figure 5.- 45° sweptback wing with the full-span leading-edge and the full-span trailing-edge flaps deflected shown mounted in the Langley full-scale tunnel.

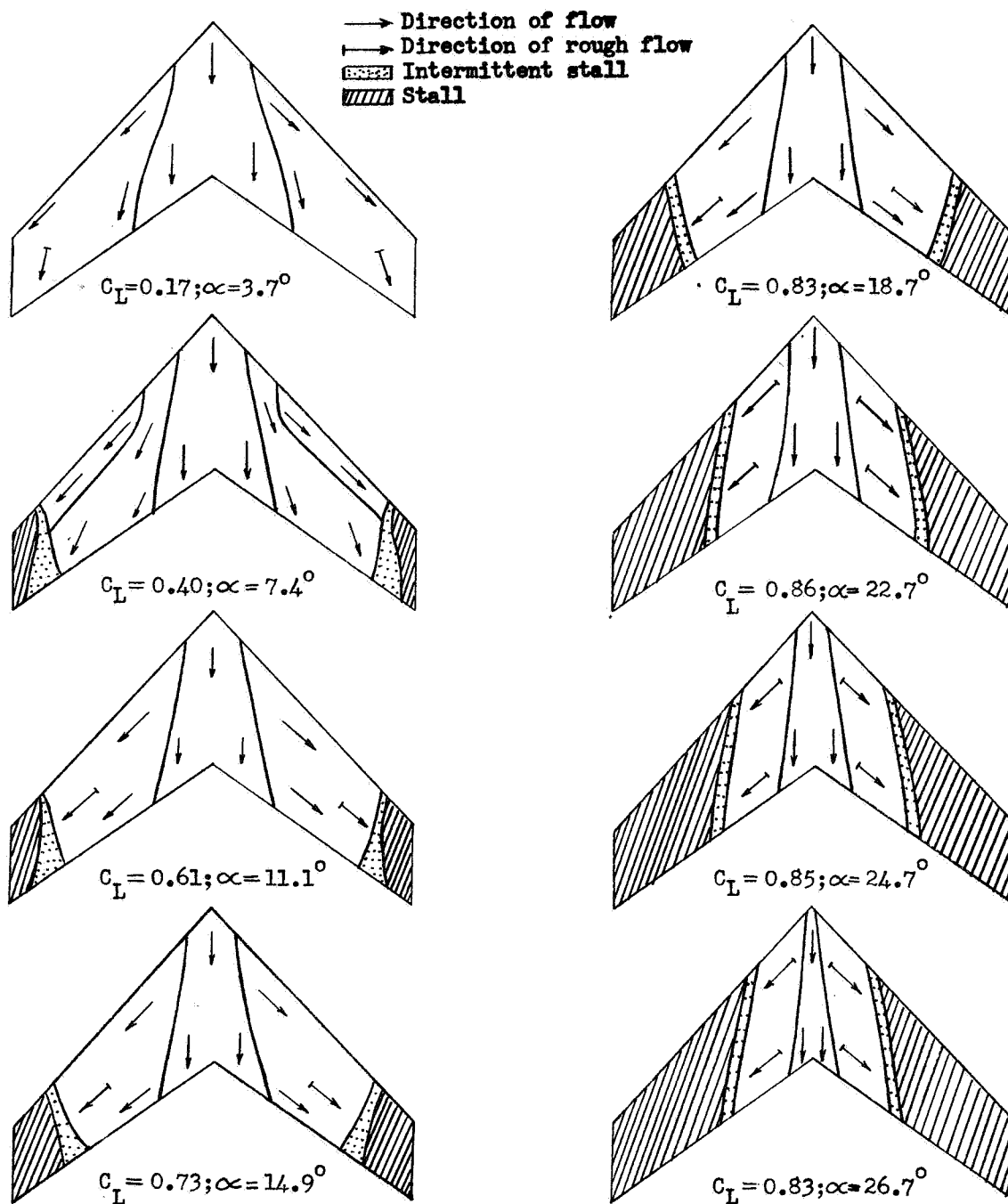


Figure 6. - Tuft studies of the wing with all flaps neutral.

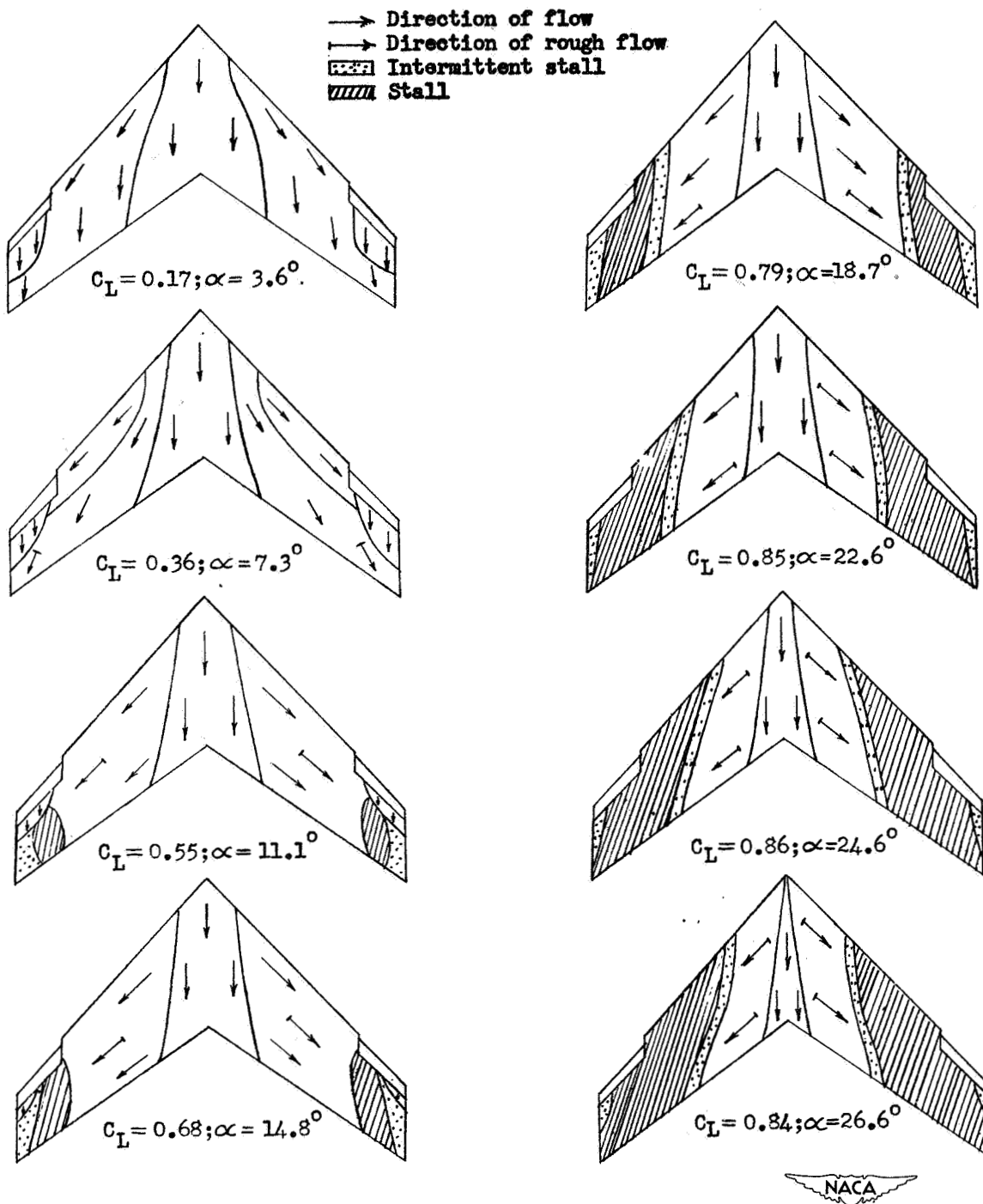


Figure 7.- Tuft studies of the wing with the outboard 25 percent of the leading-edge flaps deflected 30° ; trailing-edge flaps neutral.

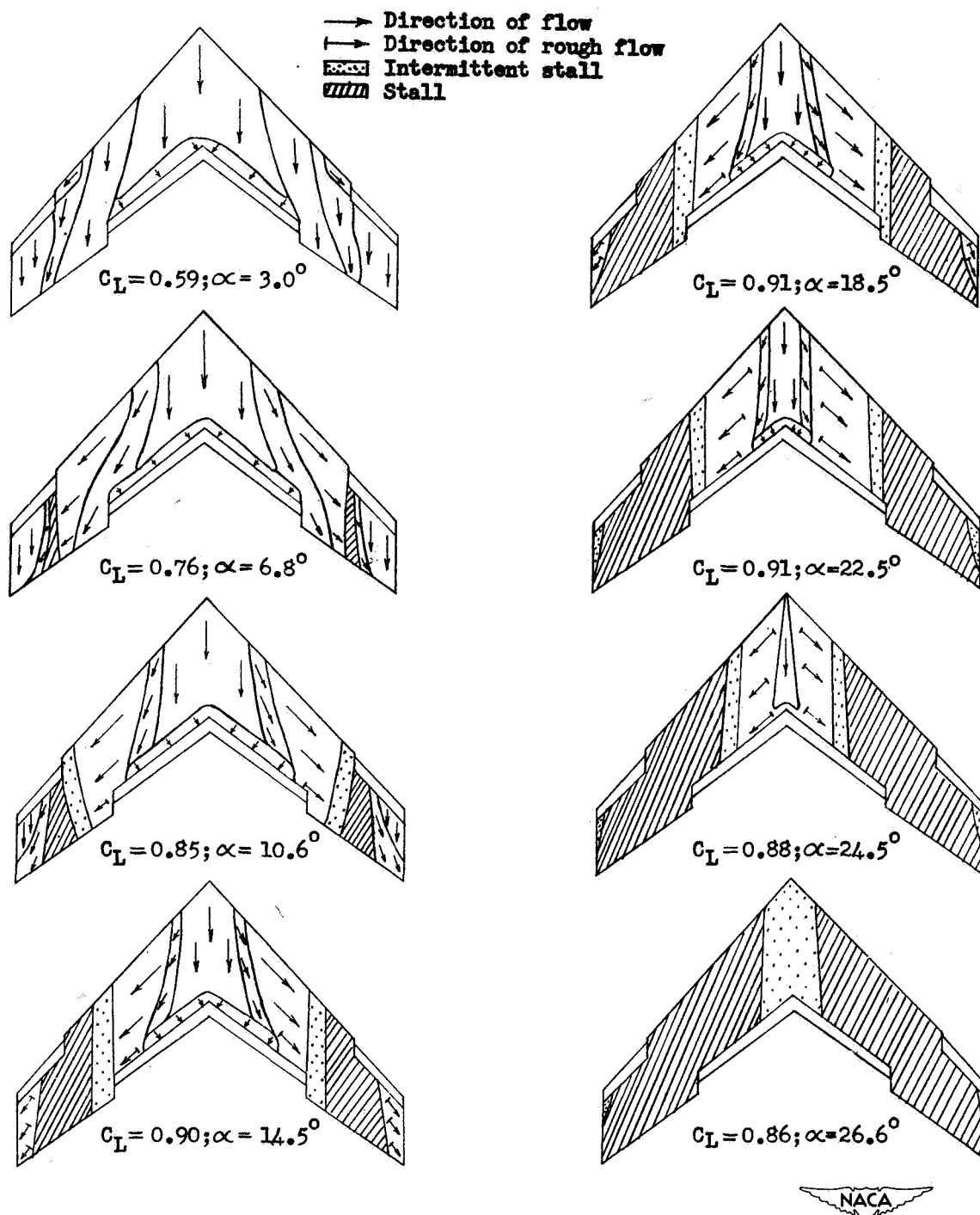


Figure 8.- Tuft studies of the wing with the outboard 25 percent of the leading-edge flaps deflected 30° , and with the inboard 50 percent of the trailing-edge flaps deflected 60° .

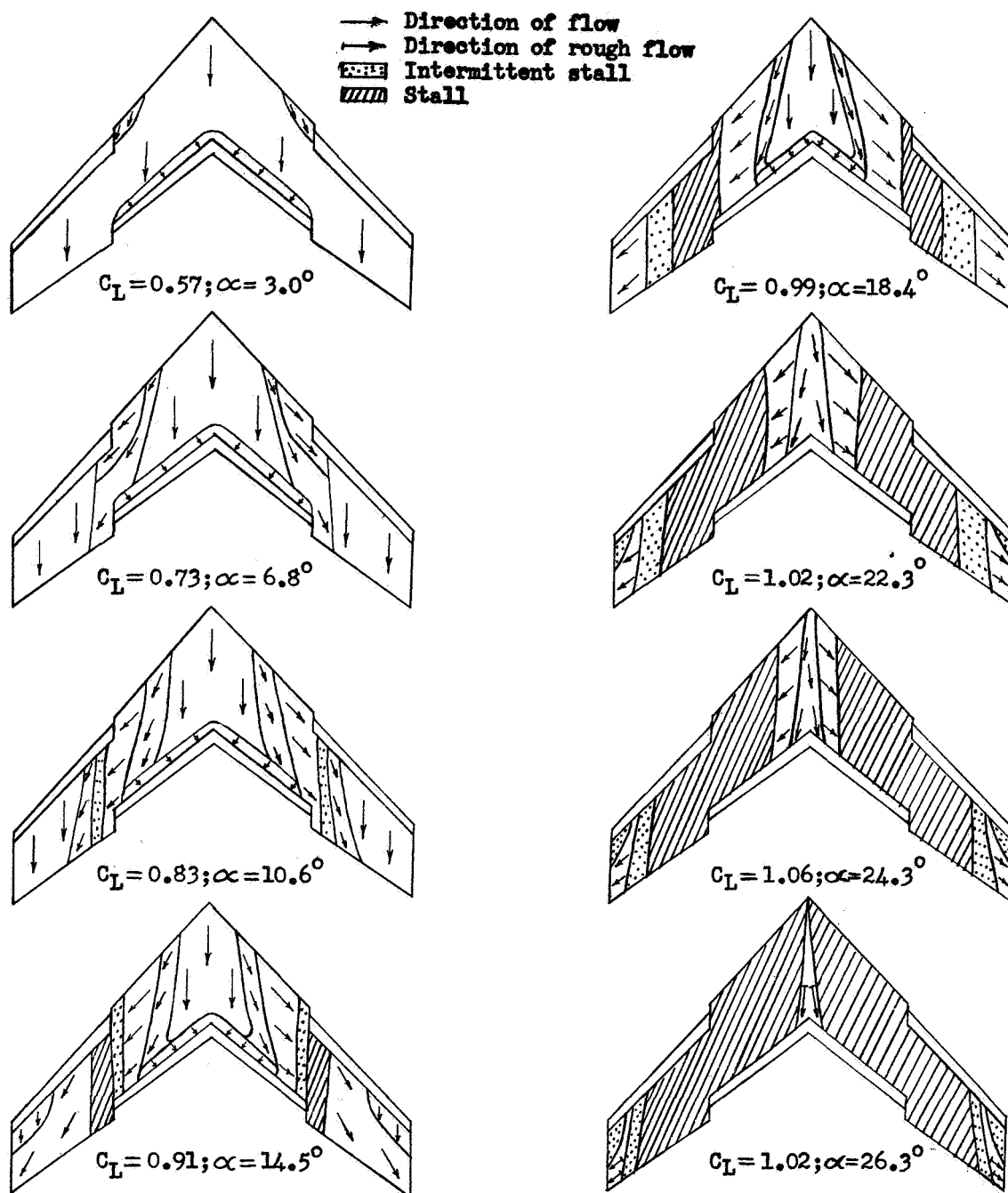


Figure 9.- Tuft studies of the wing with the outboard 50 percent of the leading-edge flaps deflected 30° , and with the inboard 50 percent of the trailing-edge flaps deflected 60° .

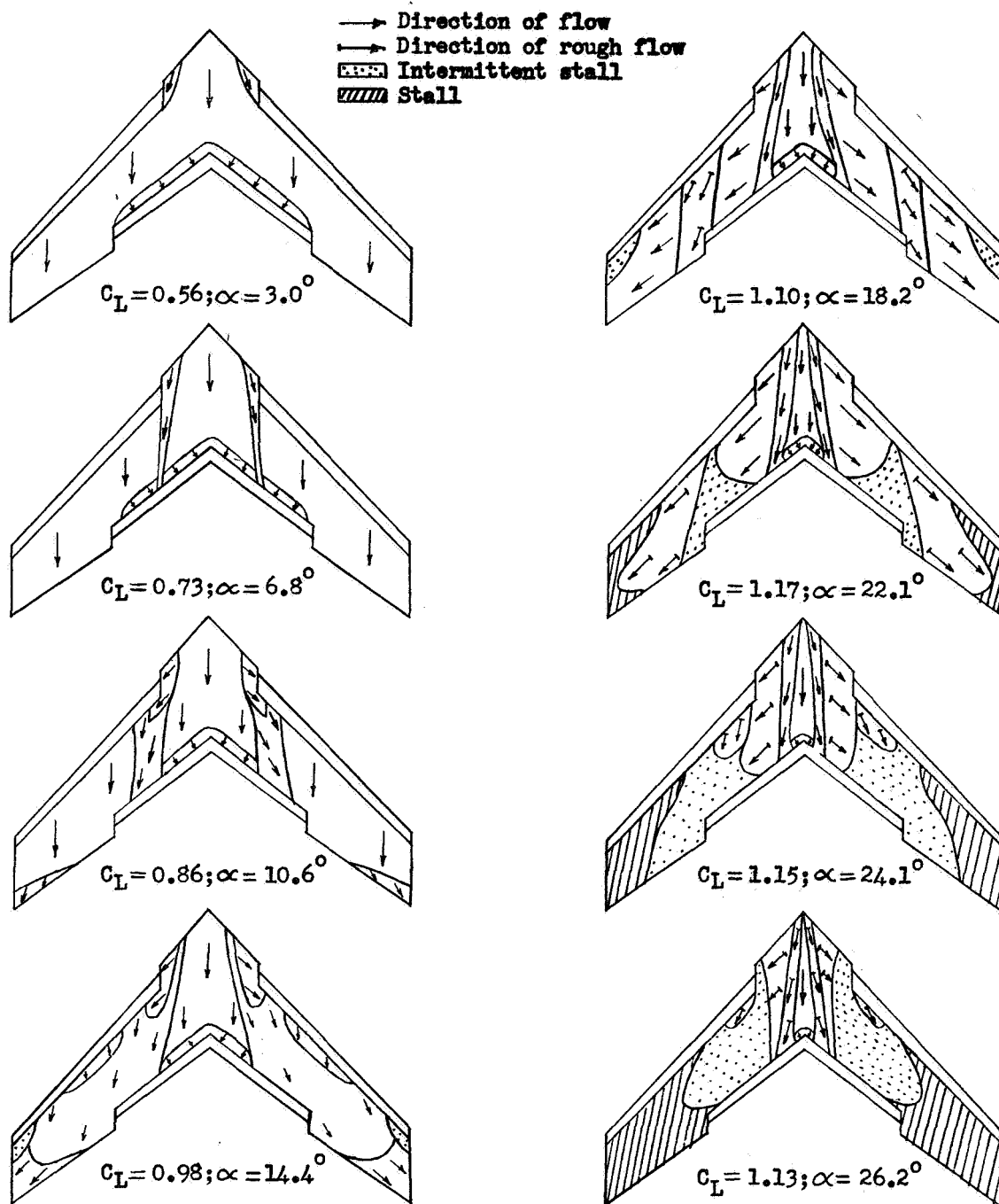
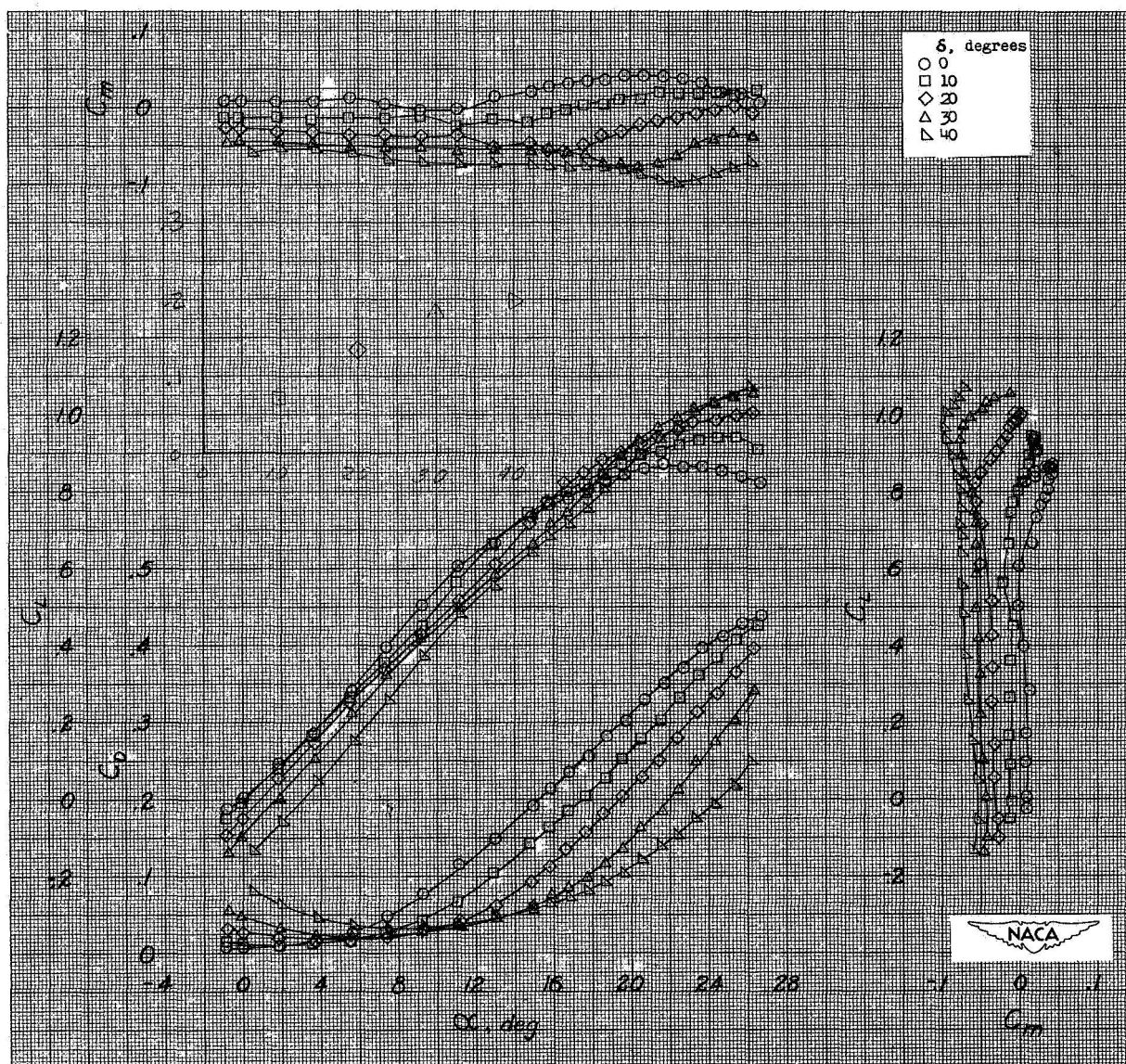


Figure 10.- Tuft studies of the wing with the outboard 75 percent of the leading-edge flaps deflected 30° , and with the inboard 50 percent of the trailing-edge flaps deflected 60° .



(a) Full-span deflection.

Figure 11.- The effect of deflecting a leading-edge flap on the aerodynamic characteristics of a 45° sweptback wing; trailing-edge flap neutral. $A=3.5$; $\lambda=0.5$; $R=4.5 \times 10^6$.

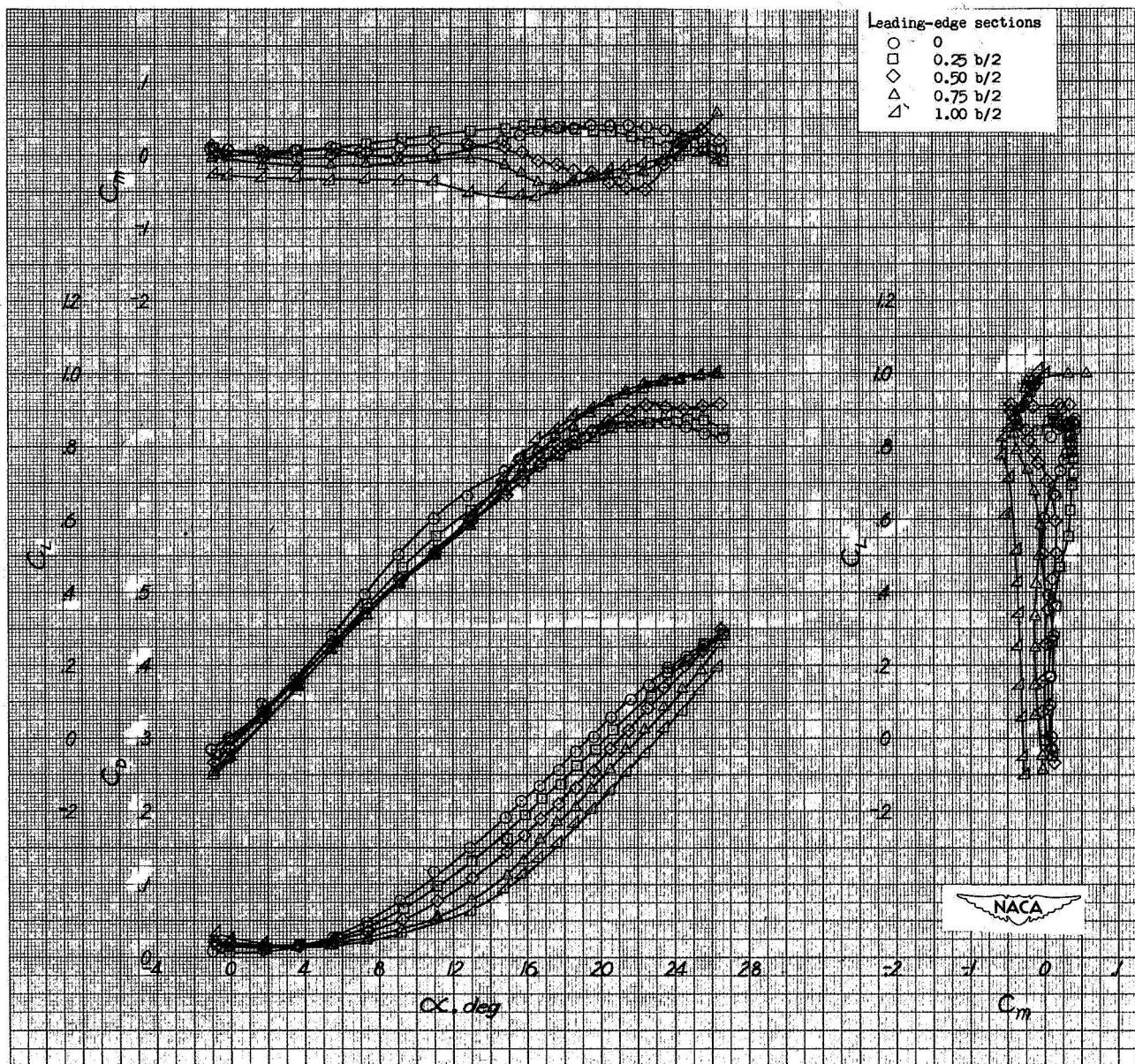
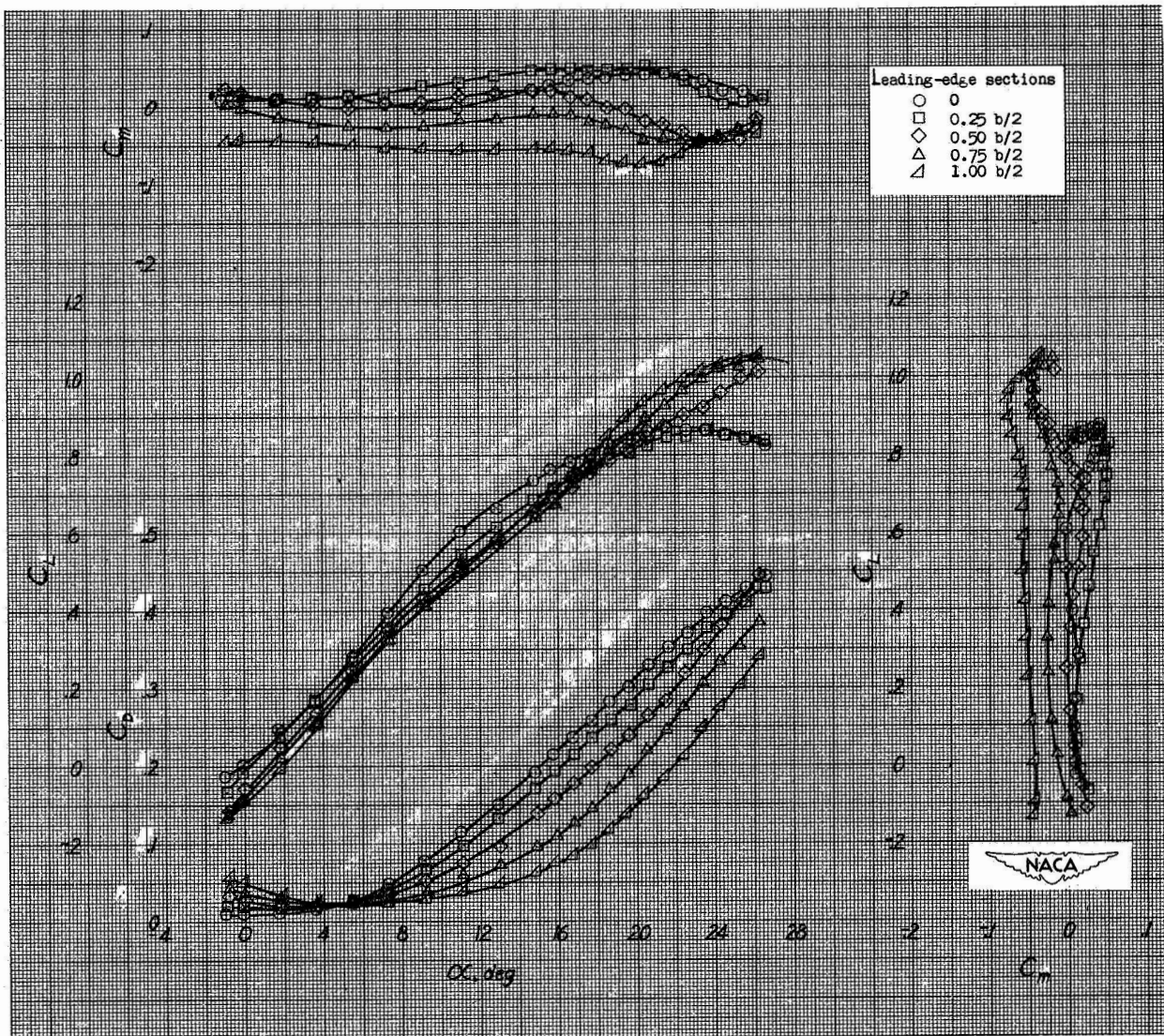
(b) Span-wise sections deflected 20° .

Figure 11.- Continued.



(c) Span-wise sections deflected 30° .

Figure 11.- Concluded.

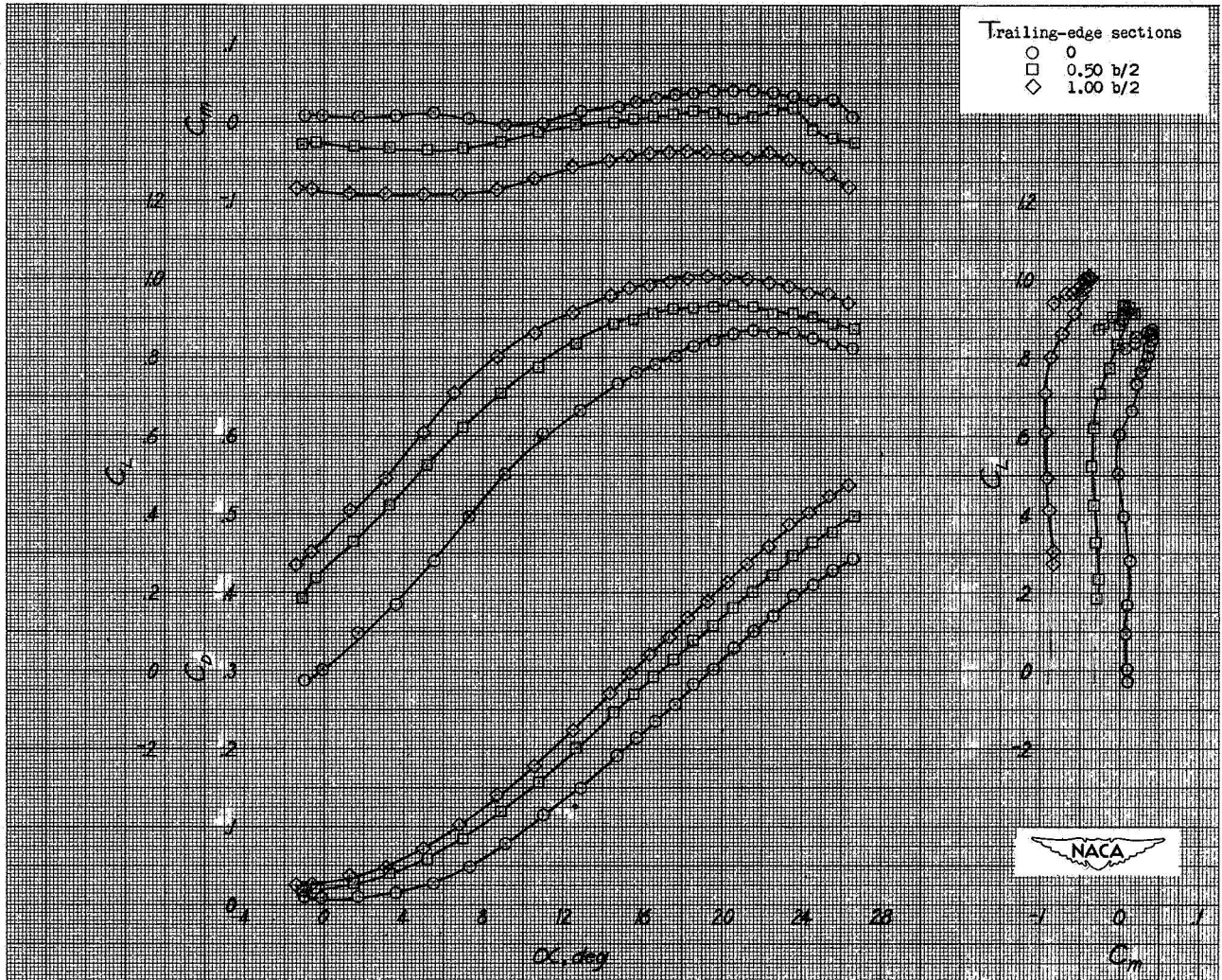
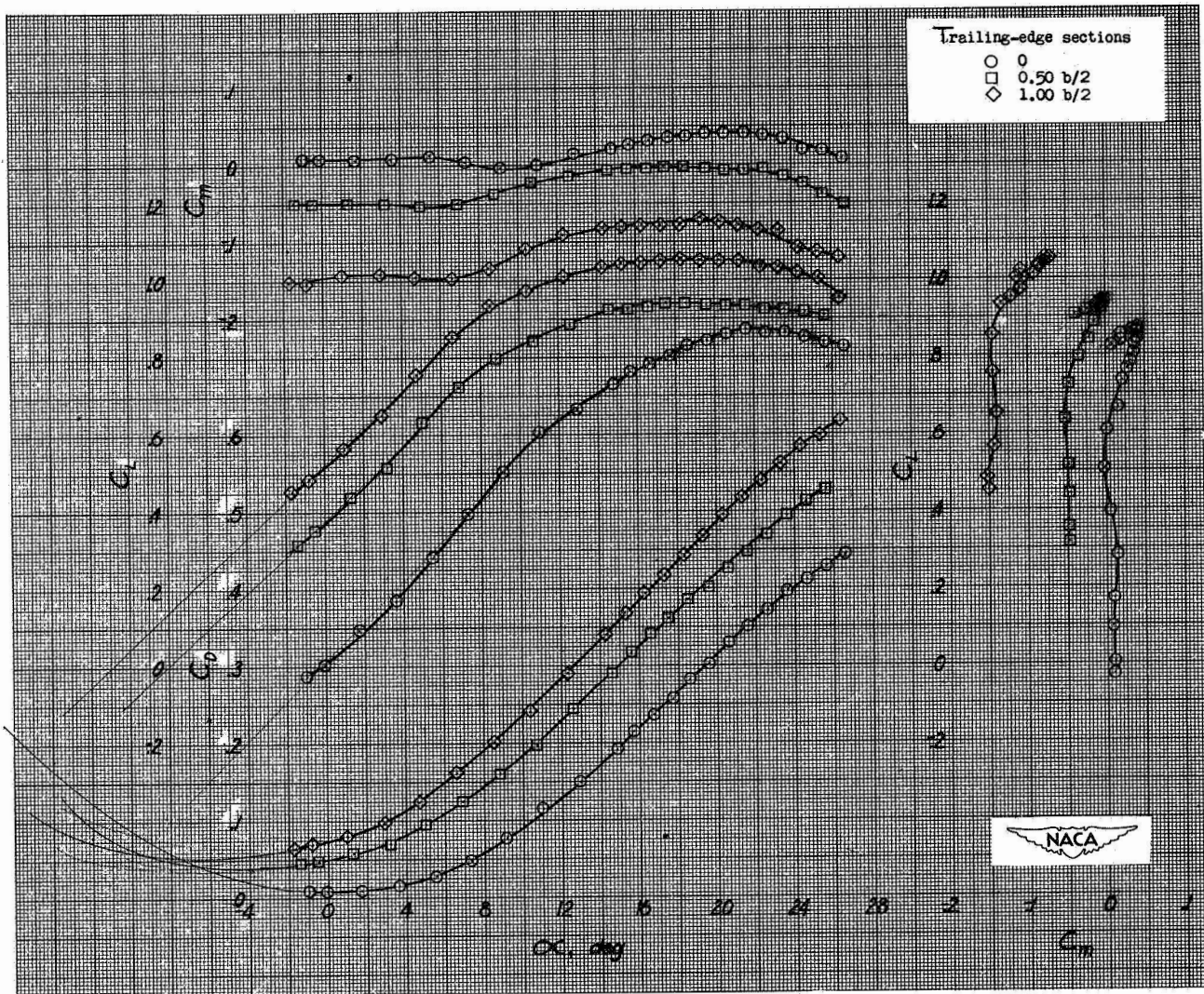
(a) Span-wise sections deflected 20° .

Figure 12.- The effect of deflecting an inboard semi-span trailing-edge flap and full-span trailing edge flap on the aerodynamic characteristics of a 45° sweptback wing; leading-edge flap neutral. $A=3.5$; $\lambda=0.5$; $R=4.5 \times 10^6$.



(b) Span-wise sections deflected 40° .
Figure 12.- Continued.

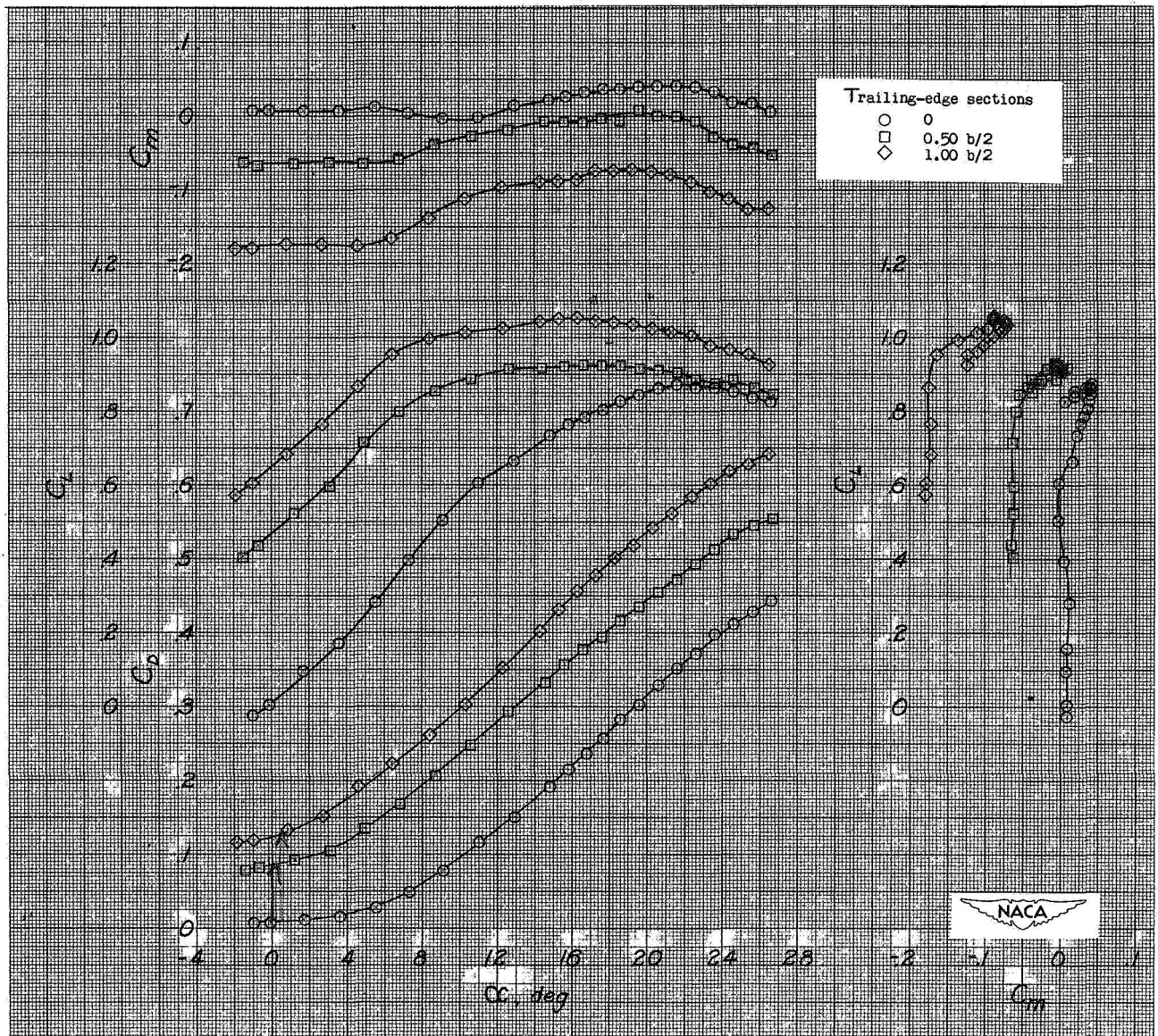
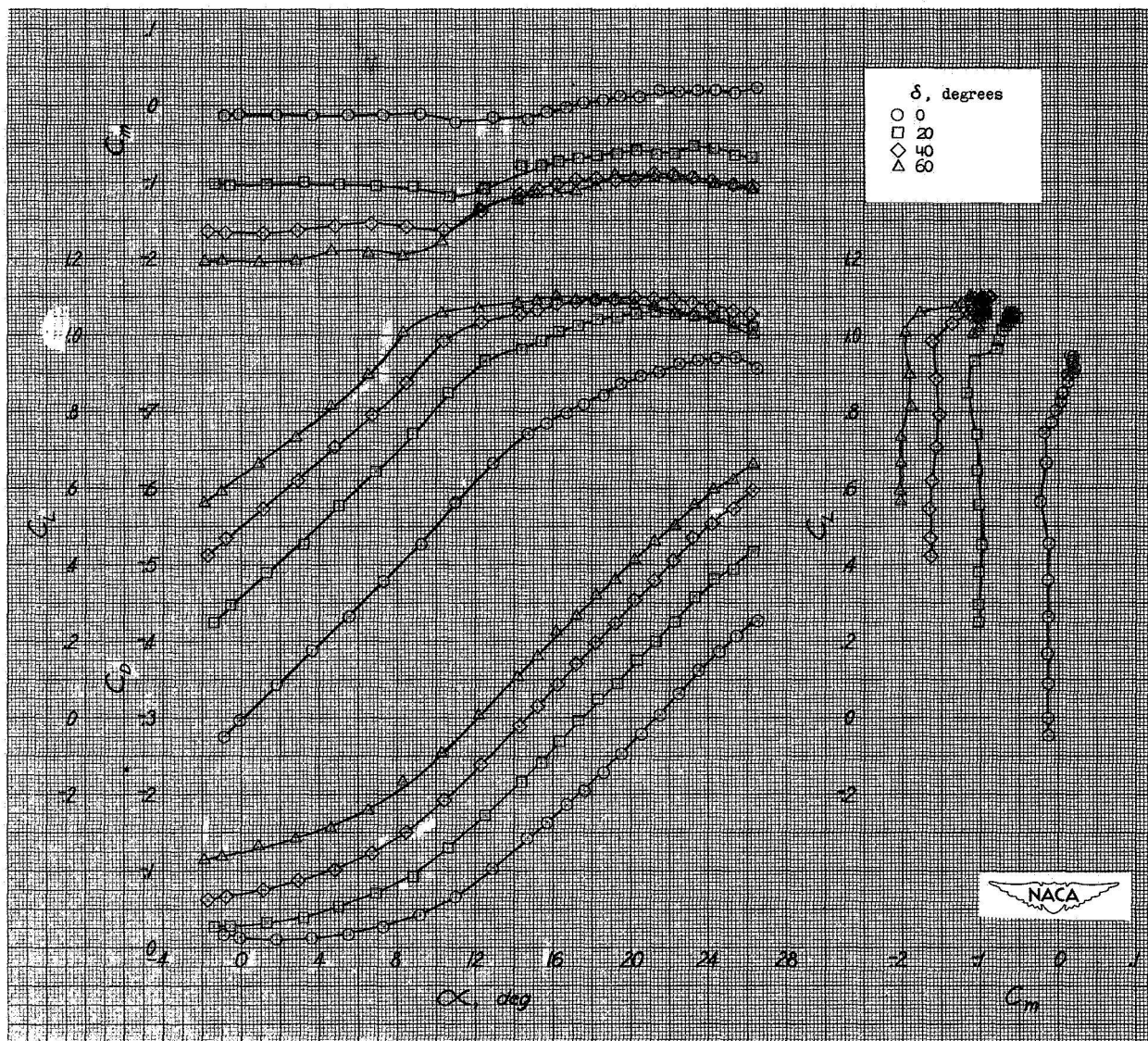
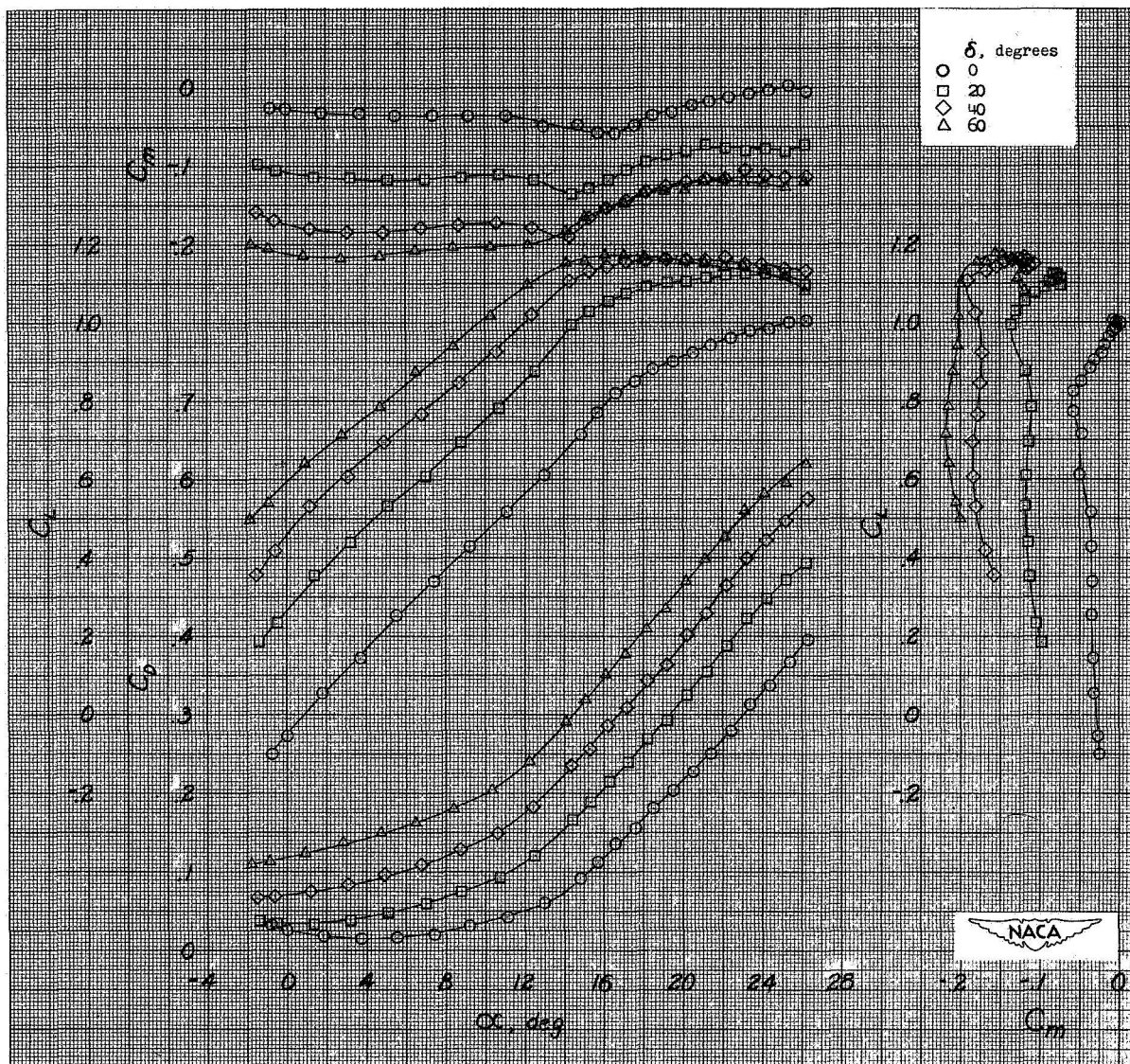
(c) Span-wise sections deflected 60° .

Figure 12.- Concluded.



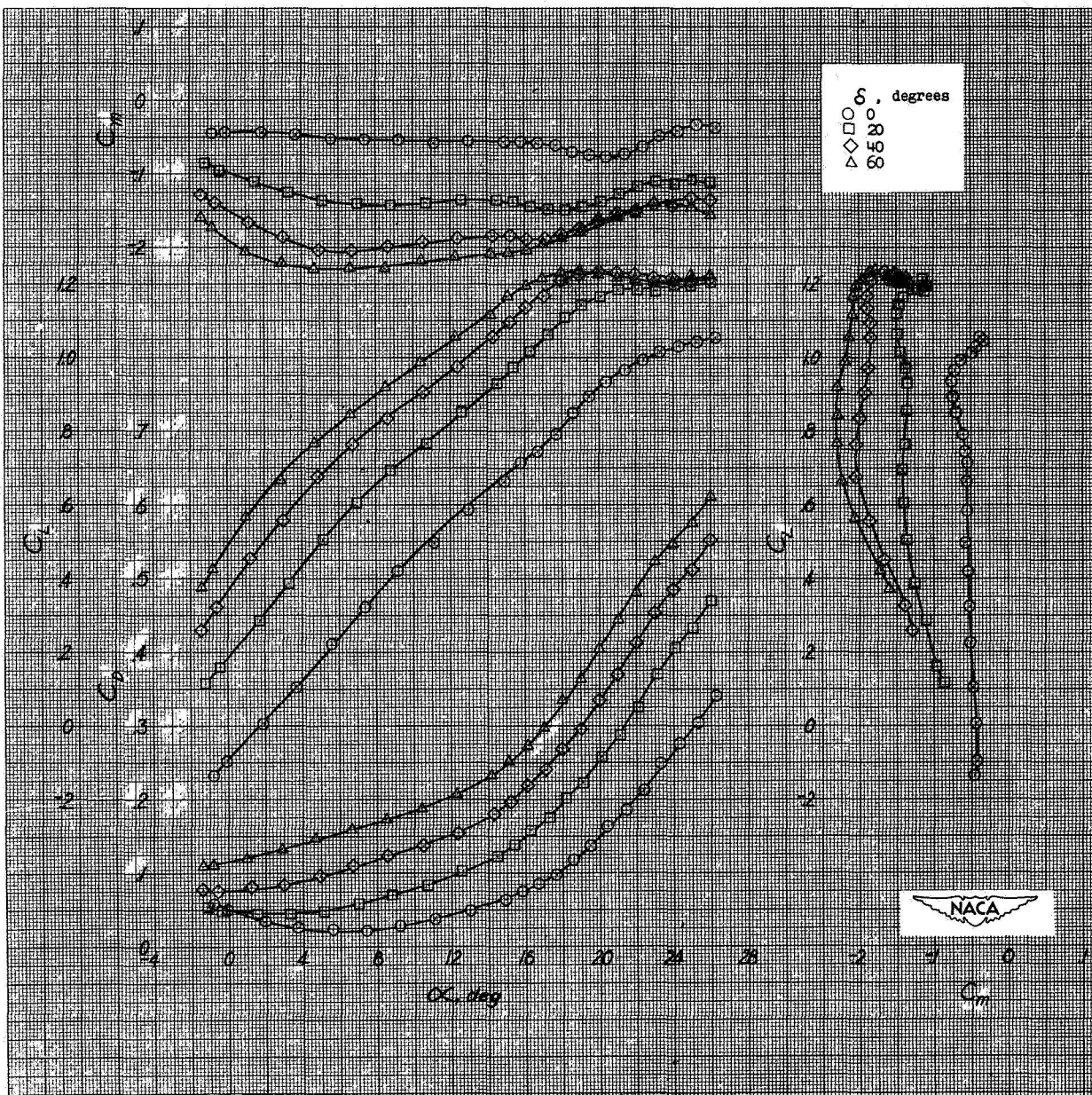
(a) Full-span leading edge flap deflected 10° ;
full-span trailing-edge flap at various
deflections.

Figure 13.- The effect of deflecting combinations of leading-edge and trailing-edge flaps on the aerodynamic characteristics of a 45° sweptback wing. $A=3.5$; $\lambda=0.5$; $R=4.5 \times 10^6$.



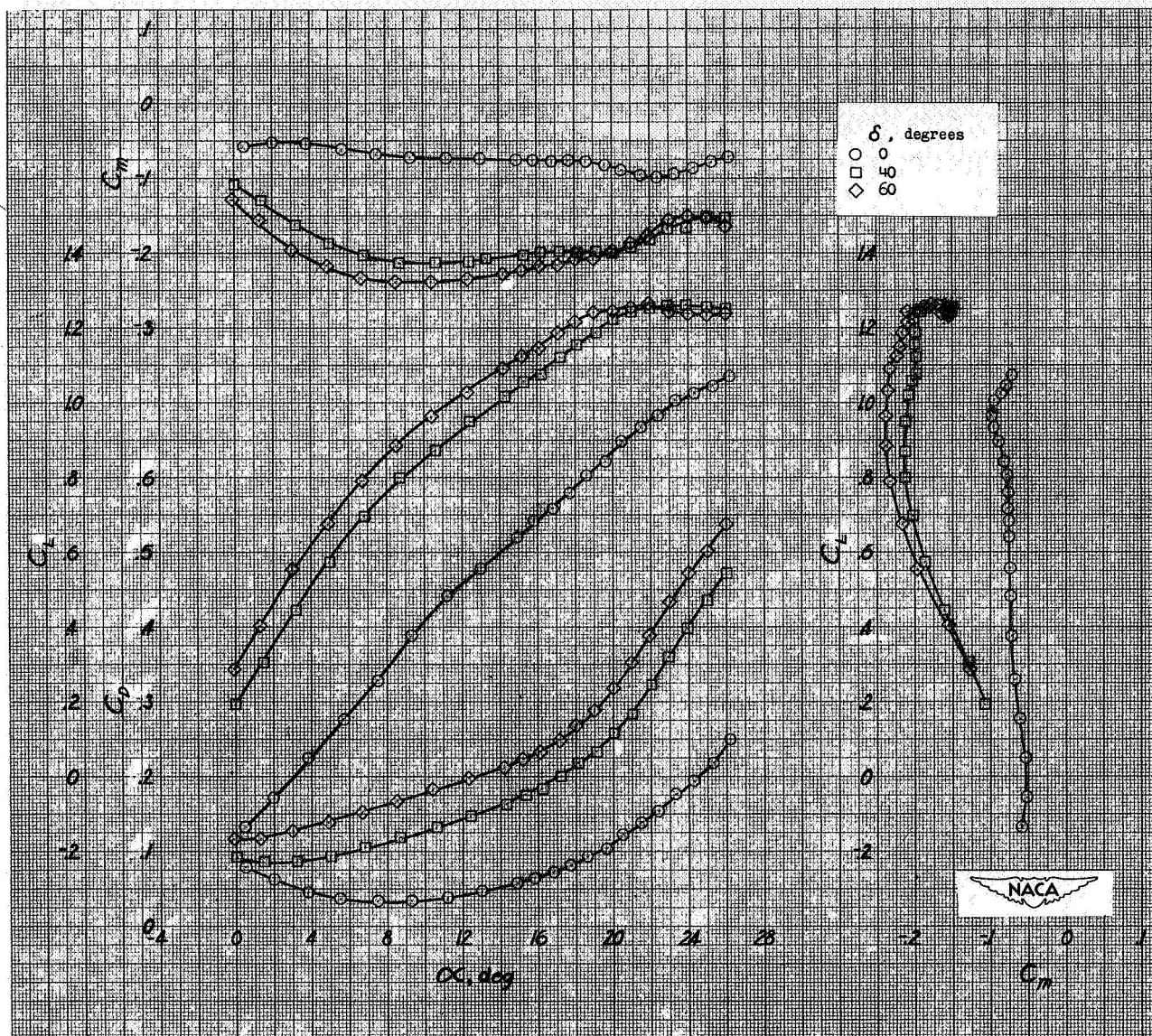
(b) Full-span leading-edge flap deflected 20° ;
full-span trailing-edge flap at various
deflections.

Figure 13.- Continued.



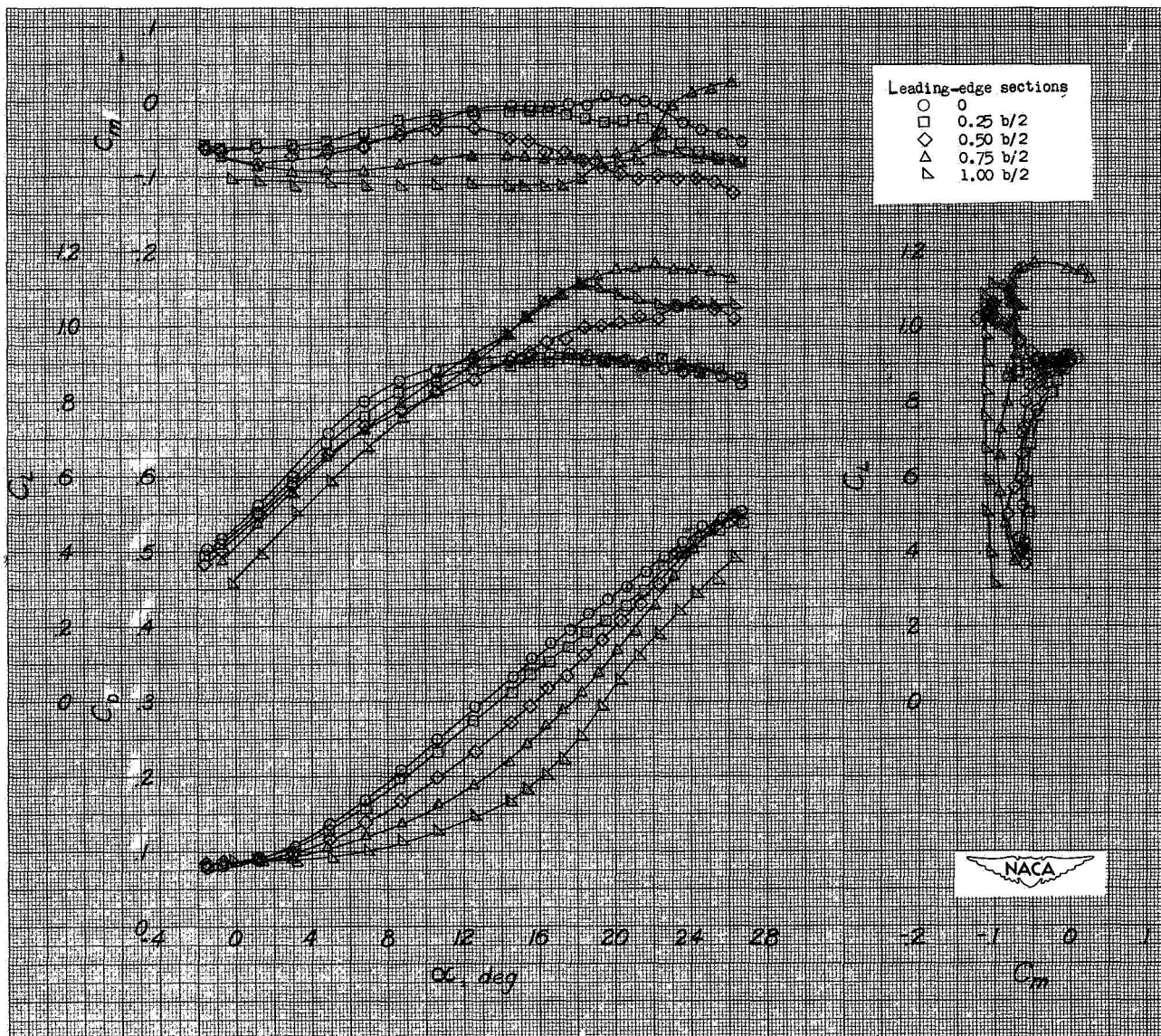
(c) Full-span leading-edge flap deflected 30° ; full-span trailing-edge flap at various deflections.

Figure 13.- Continued.



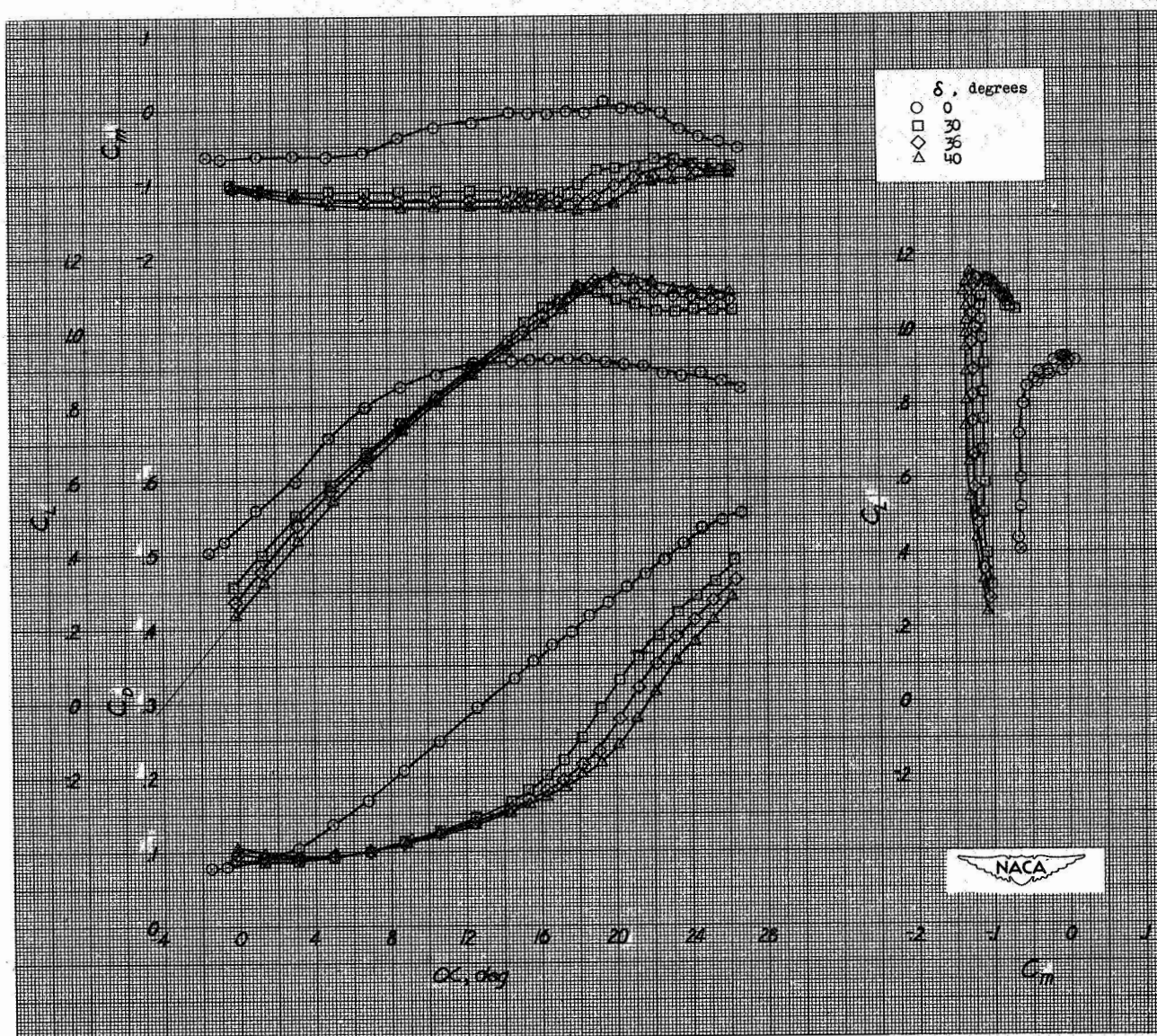
(d) Full-span leading-edge flap deflected 40° ; full-span trailing-edge flap at various deflections.

Figure 13.- Continued.



(e) Span-wise leading-edge sections deflected 30° ; inboard semi-span trailing-edge flap deflected 60° .

Figure 13.- Continued.



(f) Full-span leading-edge flap at various deflections;
inboard semi-span trailing-edge flap deflected 60° .

Figure 13.- Concluded.

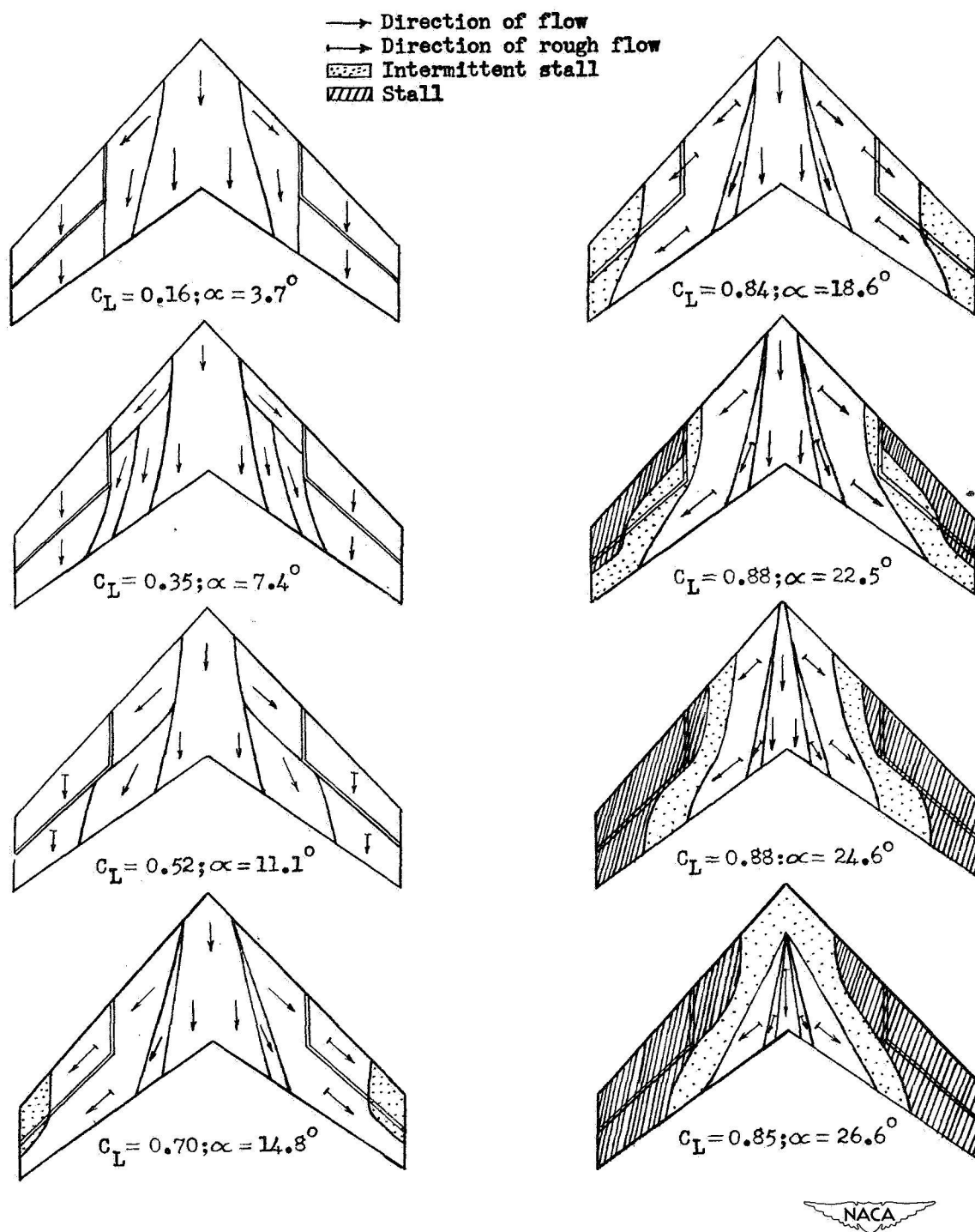


Figure 14.- Tuft studies of the wing with the rounded leading-edge installed on the outer 50-percent of the wing. All flaps neutral.

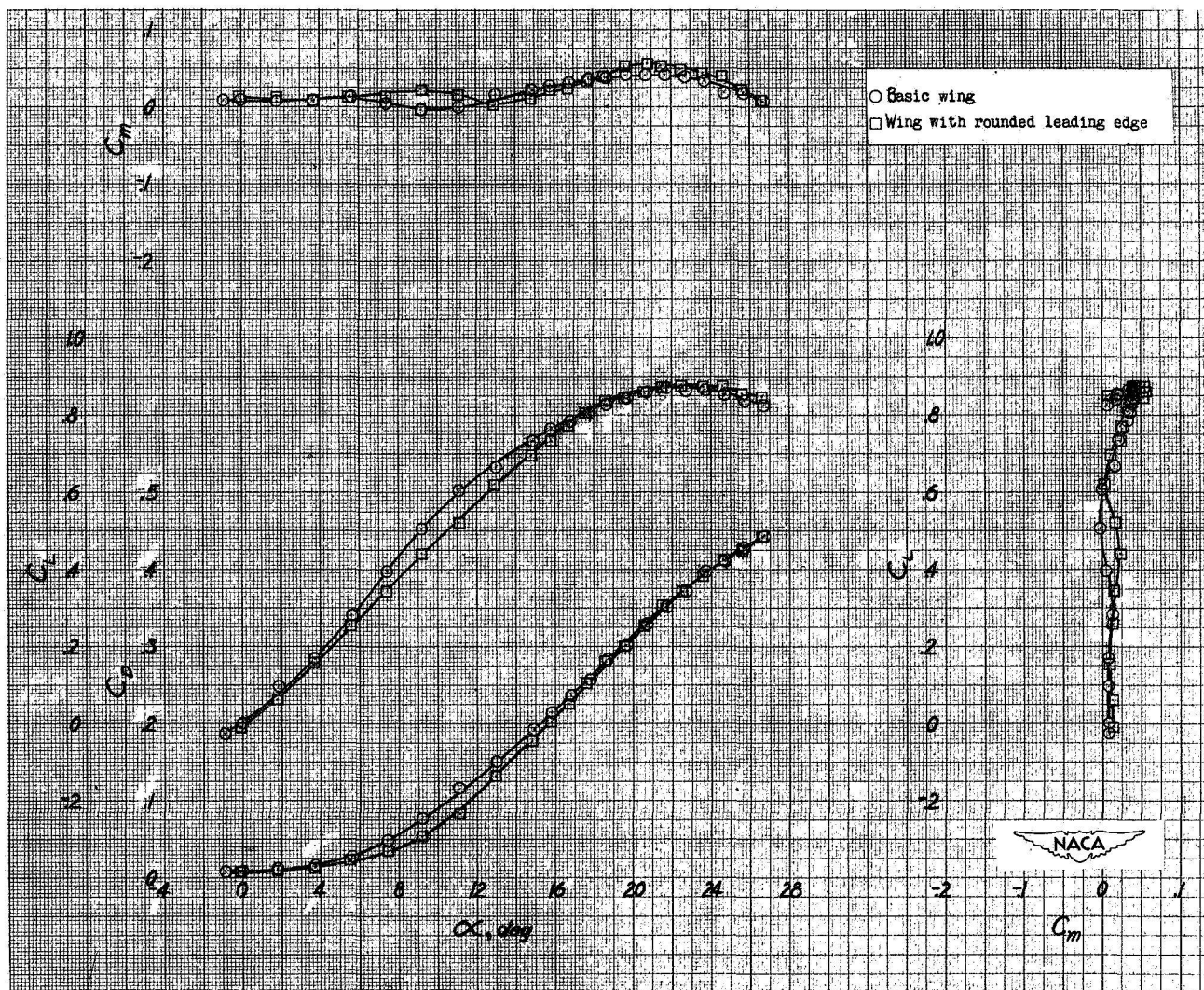


Figure 15.- The effect of an outer semi-span rounded leading edge on the aerodynamic characteristics of a 45° sweptback wing; all flaps neutral. $A=3.5$; $\lambda=0.5$; $R=4.5 \times 10^6$.

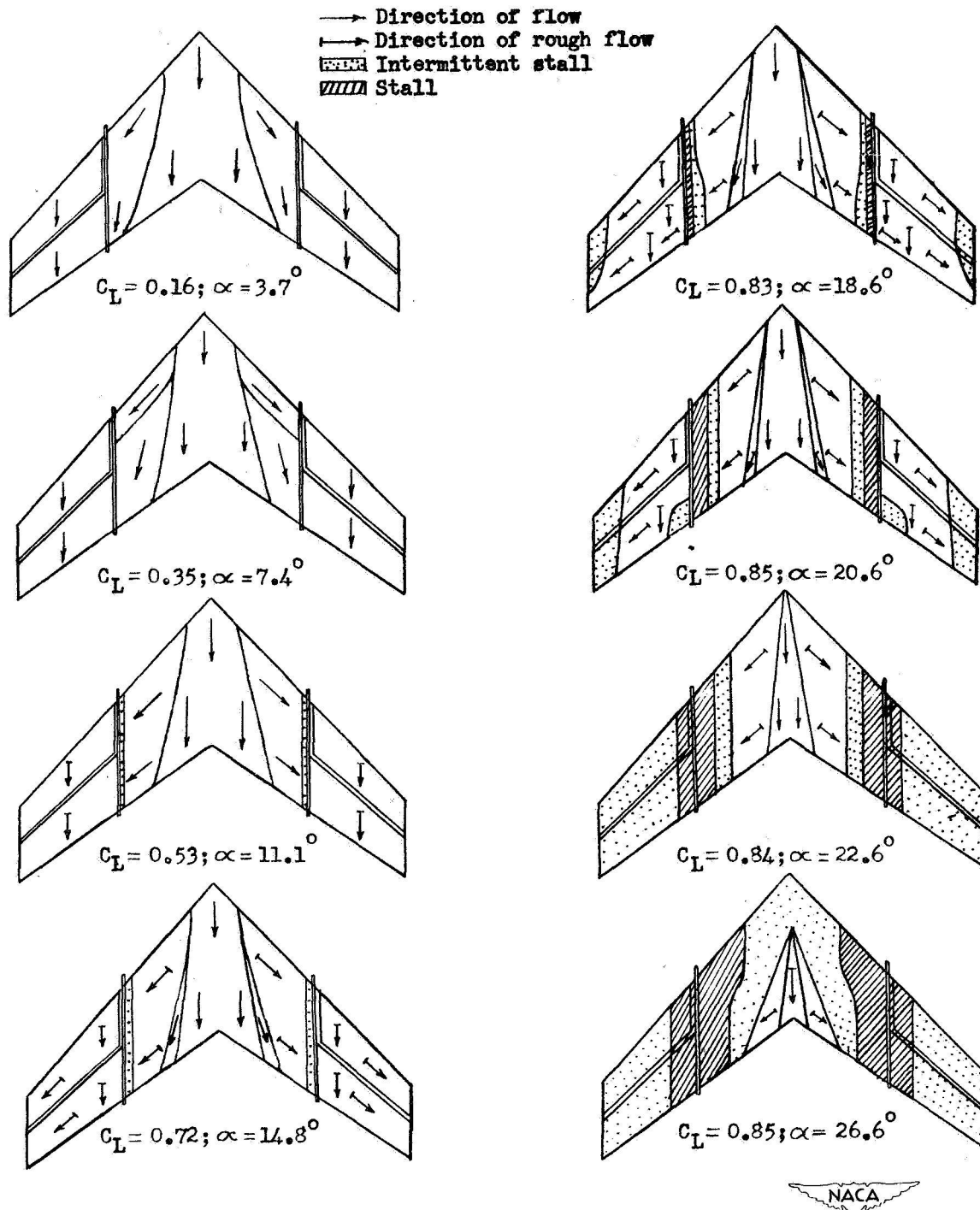


Figure 16.- Tuft studies of the wing with the rounded leading-edge installed on the outer 50-percent of the wing. Full-chord fences at the 50-percent station, all flaps neutral.

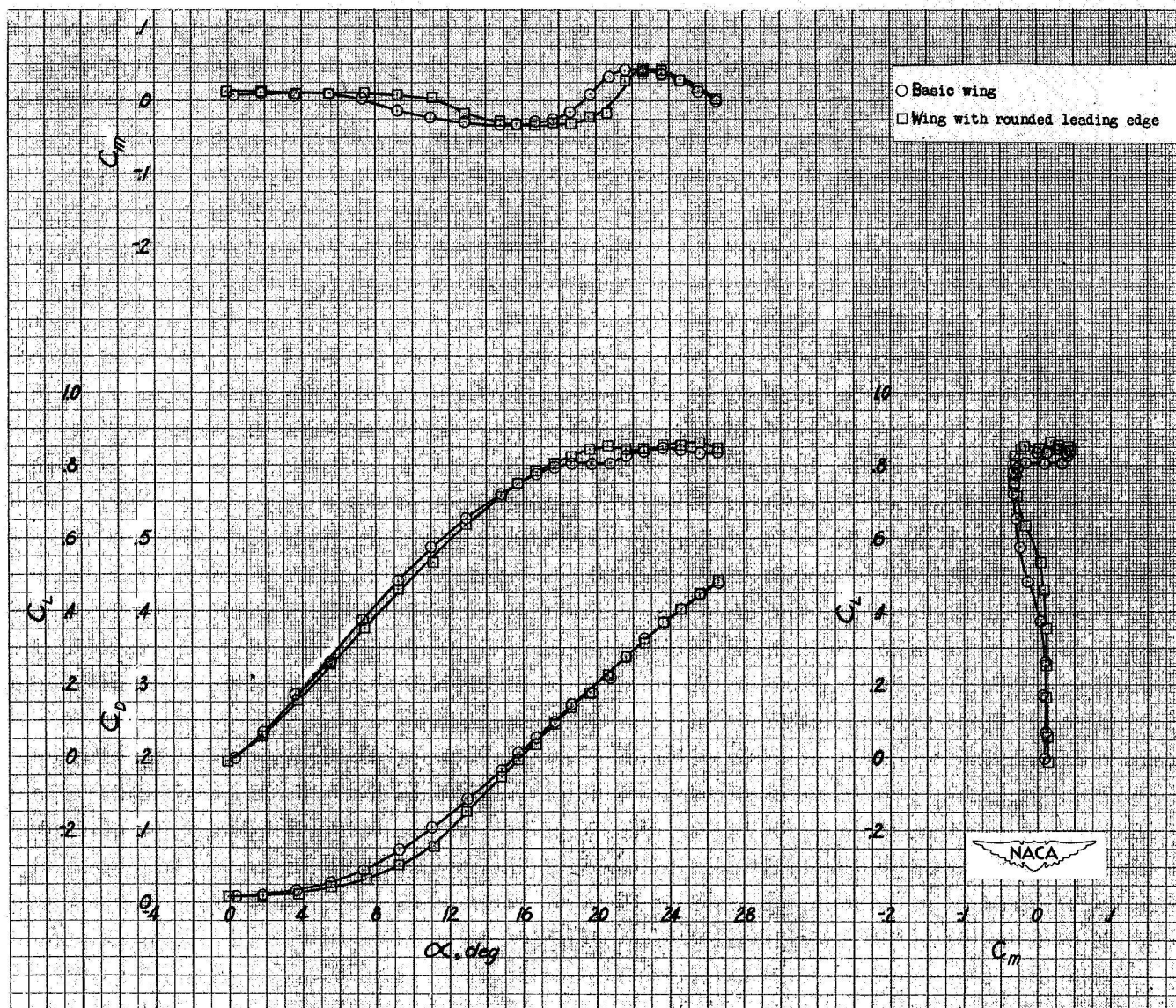


Figure 17.- The effect of fences at the 0.50 $b/2$ station on the aerodynamic characteristics of a 45° sweptback wing with and without an outer semi-span rounded leading edge installed; all flaps neutral. $A=3.5$; $\lambda=0.5$; $R=4.5 \times 10^6$.

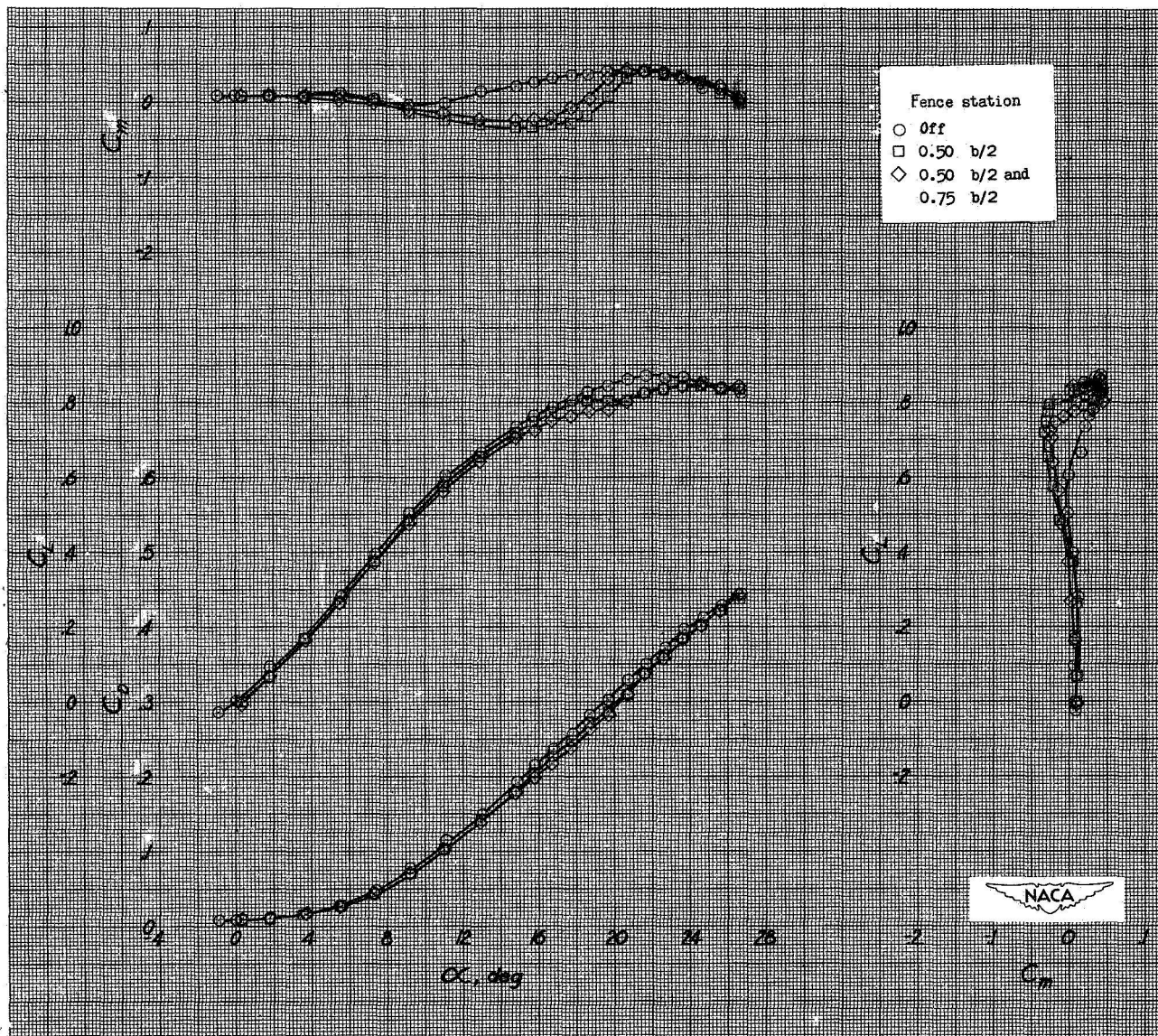


Figure 18.- The effect of fences at the 0.50 $b/2$ and the 0.75 $b/2$ stations on the aerodynamic characteristics of a 45° sweptback wing; all flaps neutral. $A=3.5$; $\lambda=0.5$; $R=4.5 \times 10^6$.

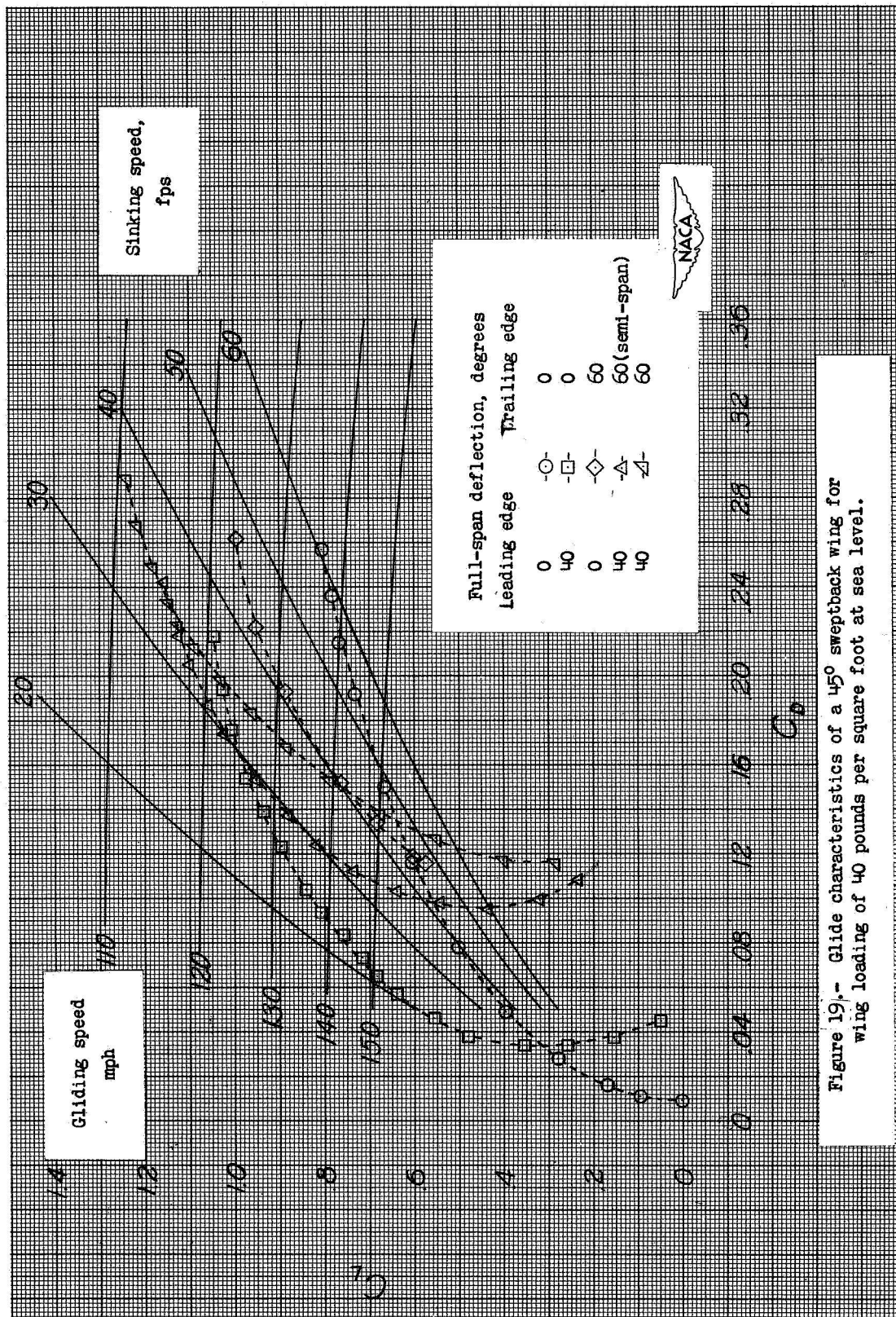
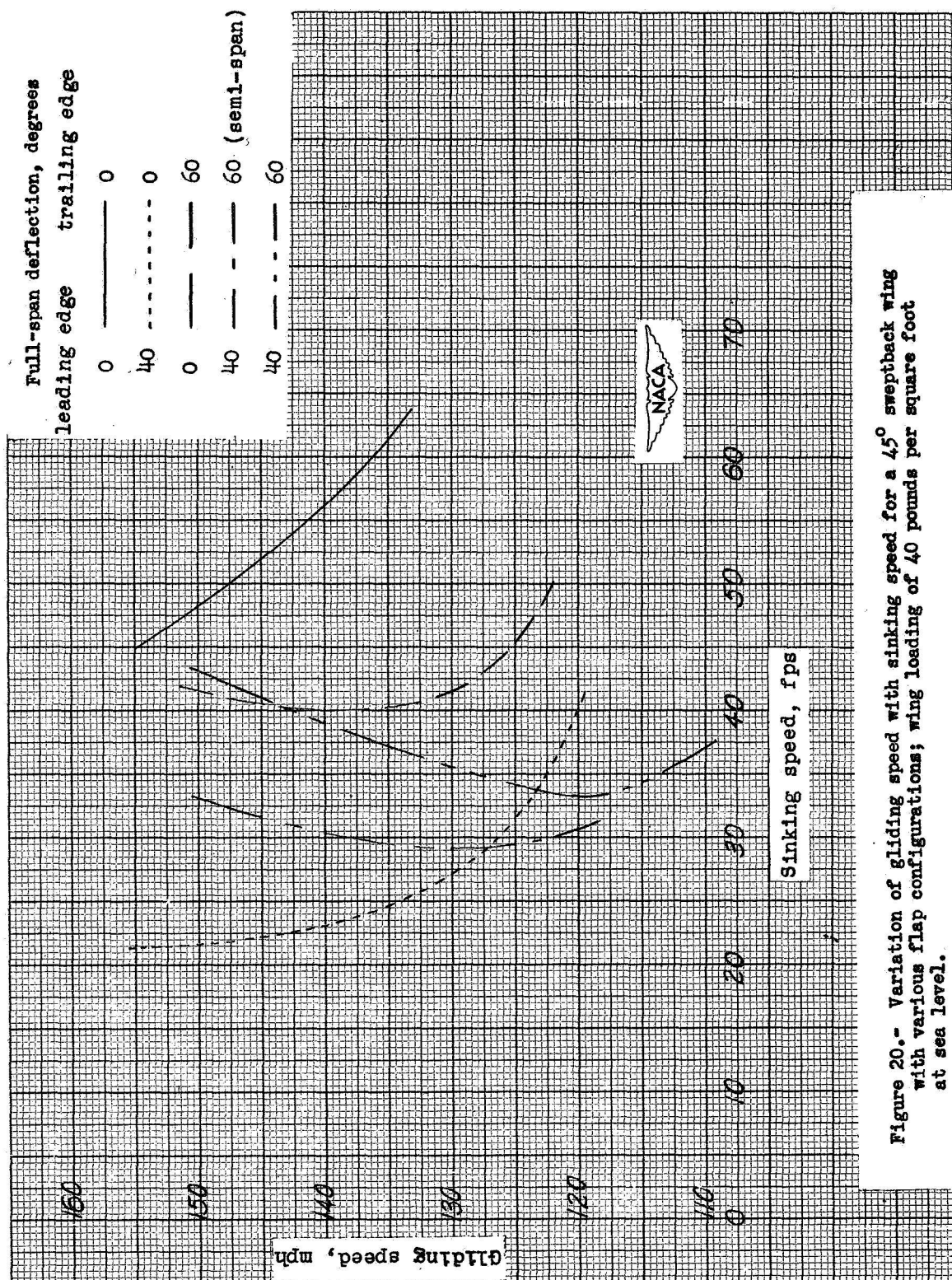


Figure 19.- Glide characteristics of a 45° sweptback wing for wing loading of 40 pounds per square foot at sea level.



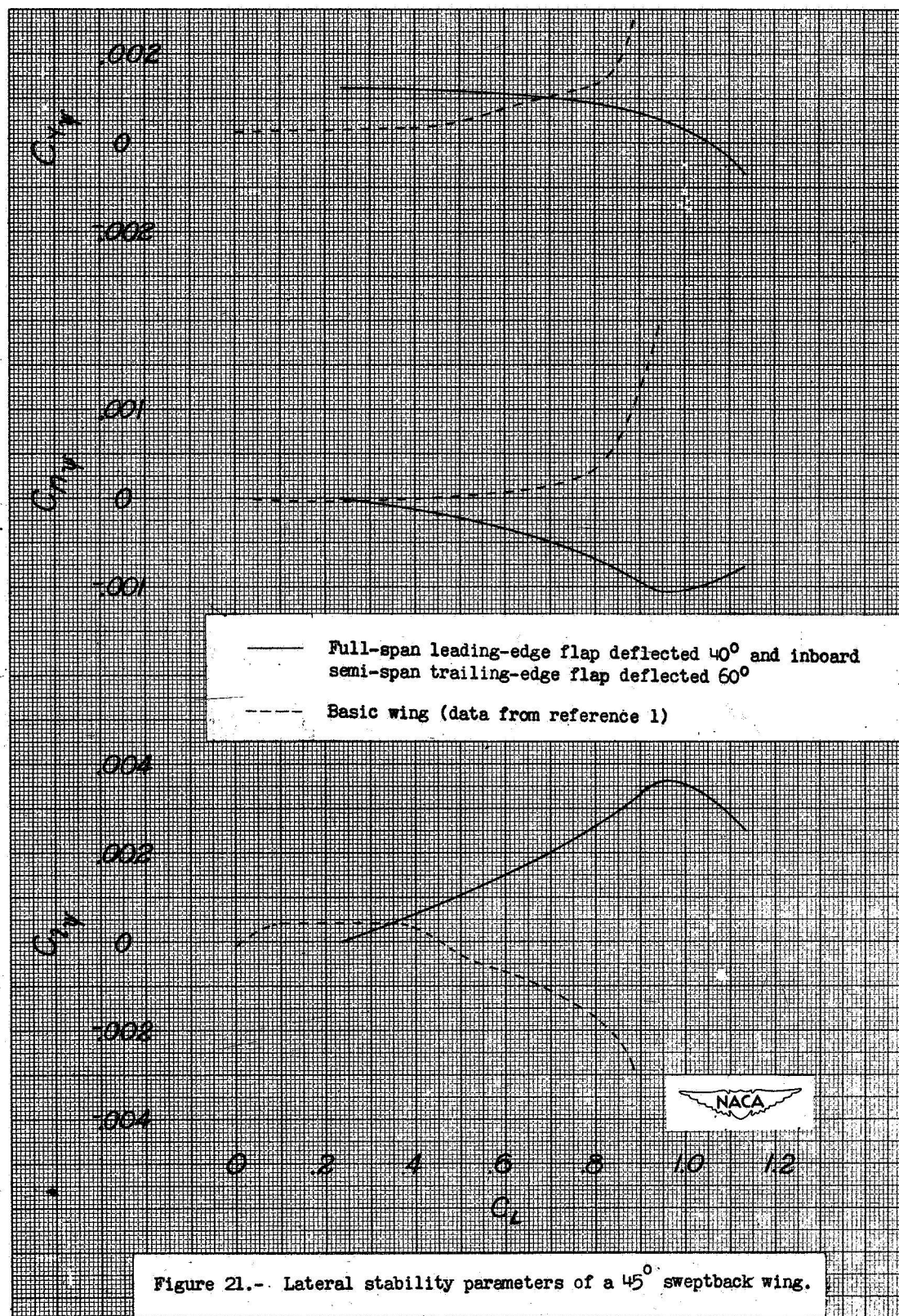


Figure 21.- Lateral stability parameters of a 45° sweptback wing.